ISSN 8755-6839

SCIENCE OF
TSUNAMI HAZARDS

The International Journal of The Tsunami Society
Volume 27 Number 2 Published Electronically 2008

THE TSUNAMI SOCIETY
P. O. Box 2117, Ewa Beach, HI 96706-0117, USA,
WWW.TSUNAMISOCIETY.ORG

OBJECTIVE: The Tsunami Society publishes this journal to increase and disseminate knowledge about tsunamis and their hazards.

DISCLAIMER: Although these articles have been technically reviewed by peers, The Tsunami Society is not responsible for the veracity of any statement, opinion or consequences.

Submit manuscripts of articles, notes or letters to the Editor. If an article is accepted for publication the author(s) must submit a scan ready manuscript, a Doc, TeX or a PDF file in the journal format. Issues of the journal are published electronically in PDF format. Recent journal issues are available at:
http://www.TsunamiSociety.org
http://www.sthjournal.org

Tsunami Society members will be advised by e-mail when a new issue is available. There are no page charges for one paper per calendar year for authors who are members of the Tsunami Society. Permission to use figures, tables and brief excerpts from this journal in scientific and educational works is hereby granted provided that the source is acknowledged.

Issues of the journal from 1982 thru 2005 are available in PDF format at
http://epubs.lanl.gov/tsunami/ and on a CD-ROM from the Society to Tsunami Society members. ISSN 8755-6839 http://www.sthjournal.org

NOAA/WEST COAST AND ALASKA TSUNAMI WARNING CENTER PACIFIC OCEAN RESPONSE CRITERIA

Paul Whitmore - NOAA/West Coast/Alaska Tsunami Warning Center - Palmer, Alaska
Harley Benz – USGS/National Earthquake Information Center - Golden, Colorado
Maiclaire Bolton – British Columbia Provincial Emergency Program - Victoria, British Columbia
George Crawford – Washington Emergency Management Division – Camp Murray, Washington
Lori Dengler – Humboldt State University – Arcata, California
Gerard Fryer – NOAA/Pacific Tsunami Warning Center – Ewa Beach, Hawaii
Jim Goltz – California Office of Emergency Services – Pasadena, California
Roger Hansen – University of Alaska, Fairbanks – Fairbanks, Alaska
Kelli Kryzanowski – British Columbia Provincial Emergency Program - Victoria, British Columbia
Steve Malone – University of Washington – Seattle, Washington
David Oppenheimer – USGS/Earthquake Hazards Team – Menlo Park, California
Ervin Petty – Alaska Division of Homeland Security and Emergency Management - Anchorage, Alaska
Garry Rogers – Geological Survey of Canada, Pacific Geoscience Centre, Sidney, British Columbia
Jay Wilson – Oregon Emergency Management –Salem, Oregon

ABSTRACT

New West Coast/Alaska Tsunami Warning Center (WCATWC) response criteria for earthquakes occurring in the Pacific basin are presented. Initial warning decisions are based on earthquake location, magnitude, depth, and - dependent on magnitude - either distance from source or pre-computed threat estimates generated from tsunami models. The new criteria will help limit the geographical extent of warnings and advisories to threatened regions, and complement the new operational tsunami product suite.

Changes to the previous criteria include: adding hypocentral depth dependence, reducing geographical warning extent for the lower magnitude ranges, setting special criteria for areas not well-connected to the open ocean, basing warning extent on pre-computed threat levels versus tsunami travel time for very large events, including the new advisory product, using the advisory product for far-offshore events in the lower magnitude ranges, and specifying distances from the coast for on-shore events which may be tsunamigenic.

This report sets a baseline for response criteria used by the WCATWC considering its processing and observational data capabilities as well as its organizational requirements. Criteria are set for tsunamis generated by earthquakes, which are by far the main cause of tsunami generation (either directly through sea floor displacement or indirectly by triggering of slumps). As further research and development provides better tsunami source definition, observational data streams, and improved analysis tools, the criteria will continue to adjust. Future lines of research and development capable of providing operational tsunami warning centers with better tools are discussed.

1. INTRODUCTION

Tsunami warning systems are different from most other natural hazard warning systems in that most systems are able to directly monitor the hazard for which they warn (for example, hurricanes, tornadoes, and solar storms). In order to provide information in a meaningful time frame, tsunami warning centers must issue warnings to the nearest coasts prior to observing the tsunami. Initial warnings are normally based on seismic data which defines the tsunami source as opposed to wave measurements which define the tsunami. However, seismic signal strength is not directly proportional to the tsunami strength. This reality induces warning centers to use conservative warning protocols when basing warnings solely on seismic data.

The NOAA/National Geophysical Data Center's Tsunami Database (2007) shows that approximately 85% of tsunamis are generated by earthquake disturbance of the sea floor. Many of the other tsunamis are generated by landslides that are often triggered by earthquake shaking. At present, seismic data are the best immediate data available to characterize an earthquake's potential to generate a tsunami prior to impact along the nearest coast.

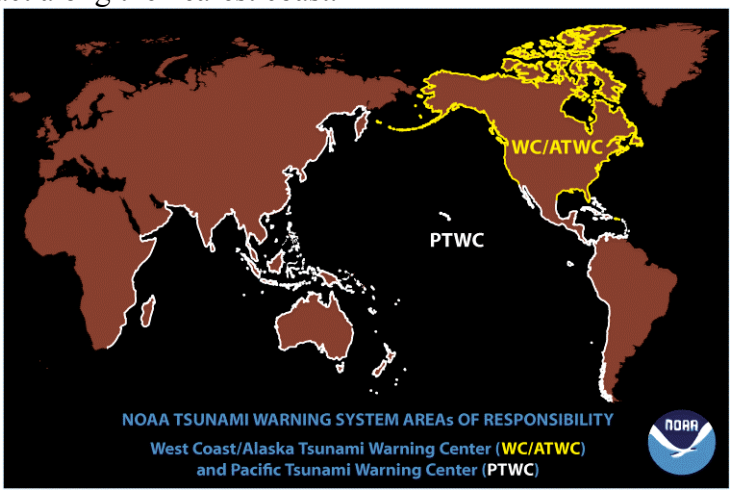

Figure 1. NOAA tsunami warning center area-of-responsibilities.

The purpose of this report is to refine criteria the warning center uses to issue tsunami messages in its Pacific area-of-responsibility (AOR – Figure 1). This AOR consists of the coasts of California, Oregon, Washington, British Columbia, and Alaska. Criteria are proposed for tsunamis generated both inside and outside the AOR. The criteria address when alerts are issued, to which areas, and what level of alert is sent. The term "alert" refers to tsunami warning, watch, and advisory which are defined later.

2. TSUNAMI WARNING CENTER OPERATIONS

Two basic types of data are recorded at tsunami warning centers: seismic and sea level. Data from approximately 300 seismometers are recorded at the WCATWC (Figure 2). The center's seismic data processing system is optimized to characterize large earthquakes as quickly as possible. Normally, the first message concerning an event is based strictly on seismic data, as the wave will not have been measured yet on a sea level gage.

After the initial bulletin is issued, seismic data are further analyzed to verify the magnitude, location, and depth, and to better characterize the event. Moment tensor solutions are computed, and - through the USGS CISNDisplay software - ShakeMaps and regional moment tensor solutions are displayed when available.

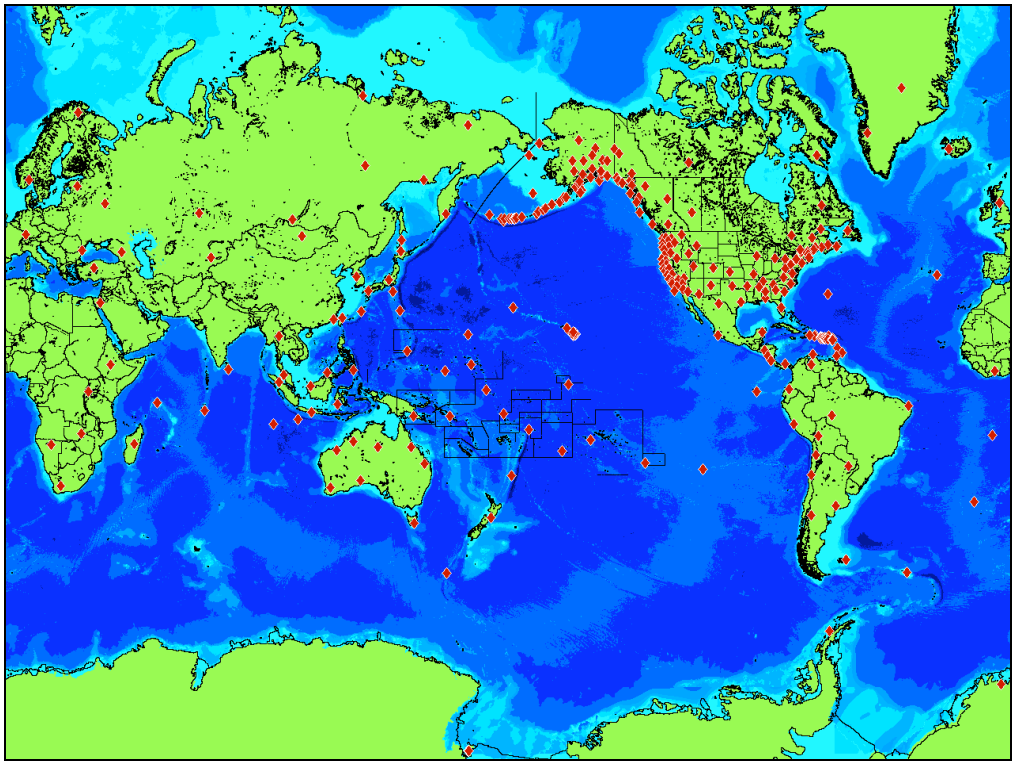

Figure 2. Diamonds represent seismometer locations recorded at the WCATWC.

Concurrent with secondary seismic data analysis, the center monitors sea level data (Figure 3). Two types of sea level data are available: coastal tide gage data and deep-ocean pressure sensor data (Deep-ocean Assessment and Reporting of Tsunamis - DART). Since 2005, the amount and quality of both tide gage data and DART data has greatly improved. These data are critical to verify the existence of tsunamis and to calibrate models used to forecast amplitudes throughout the basin. Depending on the source location, it can take anywhere from 30 minutes to 3 hours to obtain sufficient sea level data to provide forecasts for wave heights outside the source zone, or to verify that no wave has occurred and cancel the alert. Within the AOR, upgraded sea level networks have dropped the verification time to 30 minutes in some regions.

The WCATWC's goal is to issue alerts in five minutes or less for events within the AOR (Figure 4). With this short response time, an analyst must quickly review events. Procedures for the initial message must be well-planned in advance and set for all potential earthquakes. Following the initial response, analyst judgment of the situation becomes a greater part of the procedures. There are literally an infinite number of different scenarios which can play out during an event, and it is impossible to set procedures for all.

For earthquakes magnitude 8 and over, the center's initial magnitude estimate is often low since the earthquake may have not finished rupture by the time the initial processing is completed. Response criteria are set conservatively enough that the initial response will get an alert to those nearest the epicenter even with an under-estimated magnitude for earthquakes of this size.

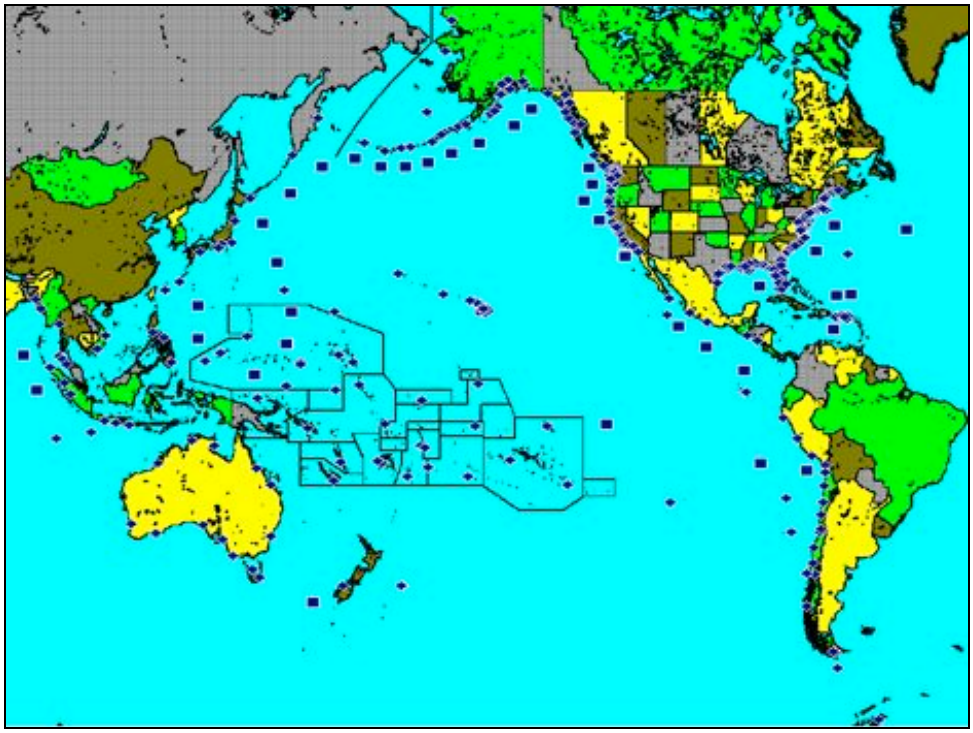

Figure 3. Diamonds represent coastal tide gages and squares represent DARTs recorded at the WCATWC.

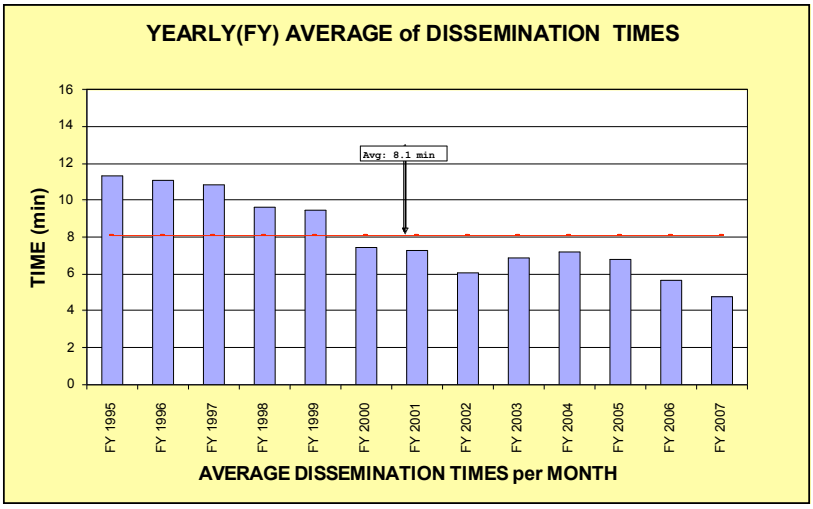

Figure 4. WCATWC response time summary. Response time is defined as the time of bulletin issuance minus the earthquake's origin time. Decrease in response time has been made possible by the use of denser, broadband seismic networks, improved seismic analysis software, and 24x7 staffing of the center.

After an alert is issued, messages are updated every 30 minutes or as necessary. In the early stages of an event, there may be no sea level data to support analysis in these supplemental messages (often the case when the event is outside the AOR). In these cases, secondary seismic analysis to better characterize the source can help guide warning center response.

Response time is mainly limited by seismic network density and distribution. For example, a center can respond in five minutes with an accurate location and magnitude if the following network criteria are met (response is defined as the time of bulletin issuance minus the origin time of the earthquake):

- 12 evenly-distributed seismic stations
- Within 900 km of the epicenter (2 minute P-wave travel time)
- 80% station uptime
- Up to 30 seconds data latency (data transmission time)
- Digital, broadband seismic data (necessary to determine moment magnitudes)

If these criteria are met, a typical timeline for warning center response would be:

- 150 seconds to record signal on 9 to 10 stations
- 60 seconds more to record enough P-wave signal for M_{wp} computations
- 30 seconds extra for final analyst review
- 60 seconds to compose and transmit appropriate message

Response timelines can be compressed by increasing seismic network density, reducing data latency, or decreasing process time. However, response time will reach a limit due to source process times for major earthquakes which can exceed 100 seconds and the fixed times of reviewing events and composing bulletins.

3. TSUNAMI WARNING CENTER MESSAGE SUITE

The WCATWC tsunami message suite has recently been revamped. In short, it has progressed from a three-level suite to a four-level suite. The products issued by the center are warning, watch, advisory, and information statement. Each has a distinct meaning relating to local emergency response. In summary:

Warning	->	Inundating wave possible	->	Full evacuation suggested
Watch	->	Danger level not yet known	->	Stay alert for more info
Advisory	->	Strong currents likely	->	Stay away from the shore
Information	->	Minor waves at most	->	No action suggested

Based on seismic data analysis or forecasted amplitude (dependent on whether the center has obtained sea level data), WCATWC will issue the appropriate product. Warnings and Advisories suggest that action be taken. Watches are issued to provide an early alert for areas that are distant from the wave front, but may have danger. Once the danger level is determined, the watch is upgraded to a warning or advisory, or canceled. The full definition of each message is given below:

Tsunami Warning - a tsunami warning is issued when a potential tsunami with significant widespread inundation is imminent or expected. Warnings alert the public that widespread, dangerous coastal flooding accompanied by powerful currents is possible and may continue for several hours after arrival of the initial wave. Warnings also alert emergency management officials to take action for the entire tsunami hazard zone. Appropriate actions to be taken by local officials may include the evacuation of low-lying coastal areas, and the repositioning of ships to deep waters when there is time to safely do so. Warnings may be updated, adjusted geographically, downgraded, or canceled. To provide the earliest possible alert, initial warnings are normally based only on seismic information.

Tsunami Watch - a tsunami watch is issued to alert emergency management officials and the public of an event which may later impact the watch area. The watch area may be upgraded to a warning or advisory - or canceled - based on updated information and analysis. Therefore, emergency management officials and the public should prepare to take action. Watches are normally issued based on seismic information without confirmation that a destructive tsunami is underway.

Tsunami Advisory - a tsunami advisory is issued due to the threat of a potential tsunami which may produce strong currents or waves dangerous to those in or near the water. Coastal regions historically prone to damage due to strong currents induced by tsunamis are at the greatest risk. The threat may continue for several hours after the arrival of the initial wave, but significant widespread inundation is not expected for areas under an advisory. Appropriate actions to be taken by local officials may include closing beaches, evacuating harbors and marinas, and the repositioning of ships to deep waters when there is time to safely do so. Advisories are normally updated to continue the advisory, expand/contract affected areas, upgrade to a warning, or cancel the advisory.

Tsunami Information Statement - a tsunami information statement is issued to inform emergency management officials and the public that an earthquake has occurred, or that a tsunami warning, watch or advisory has been issued for another section of the ocean. In most cases, information statements are issued to indicate there is no threat of a destructive tsunami and to prevent unnecessary evacuations as the earthquake may have been felt in coastal areas. An information statement may, in appropriate situations, caution about the possibility of destructive local tsunamis. Information statements may be re-issued with additional information, though normally these messages are not updated. However, a watch, advisory or warning may be issued for the area, if necessary, after analysis and/or updated information becomes available.

4 TSUNAMI AMPLITUDE VERSUS IMPACT

One important factor in determining which type of alert to issue is the impact expected from a certain size tsunami. Here, tsunami size is described by amplitude, or the level of the wave above normal sea level. Historic tide gage recordings or measured runup (the highest vertical extent of the wave along the shore) along with corresponding damage provides a relationship between amplitude and impact. Table 1 shows a comparison of recorded tide gage amplitudes or measured runups and corresponding damage along the U.S. west and Alaskan coasts.

Amplitude (m)	Location/Damage	Year
0.35	Shemya, AK; no damage	1996
0.4	Santa Barbara, CA; no damage	2006
0.4	Yakutat, AK; no damage	1987
0.45	Shemya, AK; no damage	2006
0.5	San Francisco, CA; strong current stops ferry	1960

0.5	Port Hueneme, CA; no damage	1957
0.5	Crescent City, CA, no damage	1994
0.5	Crescent City, CA; 1 mooring broke loose	1963
0.5+	San Diego, CA; boat/dock damage	1957
0.51	Adak, AK; no damage	1996
0.55	Port Orford, OR; no damage	2006
0.6	Arena Cove, CA; no damage	2006
0.6	Port San Luis, CA; no damage	2006
0.6	Ketchikan, AK; no damage	1964
0.6	Los Angeles, CA; $200K damage to boats	1964
0.6	Monterrey, CA; 2 almost drowned	1957
0.6	Crescent City, CA, no damage	1968
0.6	San Diego, CA; strong current, boat damage	1964
0.7	Crescent City, CA; no damage	1957
0.7	San Diego, CA; boat/pier damage (20 knot current)	1960
0.8	Unga, AK; dock washed away	1946
0.8	Port Hueneme, CA; railroad tracks flooded	1946
0.8	San Pedro, CA; wharf flooded	1868
0.8	Avila, CA; no damage	1927
0.8	Santa Barbara, CA; no damage	1946
0.8	Santa Barbara, CA; boat damage	1964
0.8+	Los Angeles, CA; $1 million damage, 1 drowning	1960
0.9	Crescent City, CA; $10M damage to docks	2006
0.9	Yakutat, AK; Mooring torn loose	1958
0.9	Adak, AK; no damage	1986
0.9	Shemya, AK; no damage	1969
0.9	Anaheim, CA; boats loose, no damage	1877
0.9	Santa Cruz, CA; boats loose, no damage	1960
0.9	Crescent City, no damage	1946
0.9	Trinidad, CA; cars stuck on beach	1992
1.0	San Pedro, CA; flooding, no damage	1877
1.0	Crescent City, CA; 4 boats sunk	1952
1.0	Cape Pole, AK; log boom broke	1960
1-1.5	San Francisco Bay, CA; $1 million damage	1964
1.1	Attu, AK; no damage	1969
1.2	Seldovia, AK; $500K damage to boats	1964
1.2	Larsen Bay, AK; warehouse flooded	1964
1.2	Annette, AK; no damage	1964
1.2	Seaside, OR; boats swept away	1946
1.4	Avila, CA; no damage	1952
1.4	Noyo River mouth, CA; several near drownings	1946
1.4	Santa Barbara, CA; much damage	1960
1.4	Ilwaco, WA; streets flooded	1964
1.4	Gearhart, OR; houses flooded	1964
1.5	Charleston, OR; no damage	1946
1.5	Taholah, WA; boats swept away	1946
1.5	Santa Cruz, CA; 1 dead, many rescued	1946
1.5	Santa Cruz, CA; minor damage	1896
1.5	Seaside, OR; boat/pier damage	1960
1.5	Stinson Beach, CA; no damage	1960
1.5	King Cove, AK; cannery damage	1946

1.6	Attu, AK; minor damage	1965
1.7	Crescent City, CA; boats sunk, pier damage, 3 injured	1960
1.8	Surf, CA; railroad station inundated	1927
1.9	Humboldt Bay, CA; some damage, flooding	1964
1.9	Adak, AK; bridge, structure destroyed	1957
2.0	Noyo Harbor, CA; boat/dock damage	1960
2.0	Noyo Harbor, CA; 10 boats sunk	1964
2.0	Copalis, WA; some injuries, much damage	1964
2.2	Half Moon Bay, CA; 3 near drownings, flooding, boat damage	1960
2.3	Umnak I. , AK; moorings destroyed	1957
2.3	Montague I. , AK; minor damage	1960
2.5	Pacific Beach, CA; injuries, damage	1964
2.6	Half Moon Bay, CA; homes flooded	1946
2.6	Drake's Bay, CA; boat capsized	1946
3.0	Santa Monica, CA; boat/pier damage	1930
3.0	Redondo Beach, CA; 1 dead, many rescued	1930
3.0	Seaside, OR; 1 dead, structural damage	1964
3.0	Cape St. Elias, AK; 1 drowned	1964
3.0+	Florence, OR; much damage	1964
3.0+	Klamath River, CA; 1 dead, some damage	1964
3.4	Gaviota, CA; ships run aground	1812
3.4	Moclips, WA; houses damaged	1964
3.5	DePoe Bay, OR; 4 deaths, some damage	1964
3.7	Yakataga, AK; no damage reported	1964
4.5	Wreck Creek, WA; minor damage	1964
4.8	Crescent City, CA; 10 dead, $15 million damage	1964

Table 1. Examples of tsunami amplitude or measured runup and resulting damage (Lander *et al.*, 1993; Lander, 1996, NGDC, 2007). Amplitudes are taken from original tide gage records where possible. There are many other recordings below 0.5m within the AOR. None of these had any associated damage.

Table 1 indicates that tsunami damage due to strong currents can occur at amplitudes as low as 0.5m. More severe damage and inundation tends to occur in the 1.5-2.0m amplitude range. Whitmore (2003) showed that tsunami amplitude forecast accuracy for events up to 1.5m amplitude is approximately 50%. This general accuracy level was also observed during the November 15, 2006 Kuril Islands tsunami for forecasts along the U.S. coast. Based on this level of accuracy, the observed amplitude/impact relationship, and the tsunami product definitions, advisories will normally be issued when forecasts are in the range 0.3m to 1.0 m and warnings when the forecast is above 1.0m.

5. WARNING CRITERIA

Tsunami response criteria can be based on historic event data. Since significant tsunamis are uncommon events, the amount of data on which to base analysis is small. Figure 5 displays tsunamis which have been recorded along the WCATWC Pacific AOR. One way to expand the data set is to use historic data from other areas in addition to the region of interest. NOAA's National Geophysical Data Center (NGDC) compiles a historic tsunami database which can be used for this purpose (NGDC 2007). Tsunami amplitudes in the database have been compared to sea level records when available and updated as necessary.

Modeling hypothetical events can also help define procedures. For example, Knight (2006) showed by modeling potential events in the Atlantic Basin, Caribbean Sea, and Gulf of Mexico that events in the Atlantic will not pose a threat to the Gulf of Mexico and vice-versa. This type of study is particularly helpful in areas with little historic tsunami information.

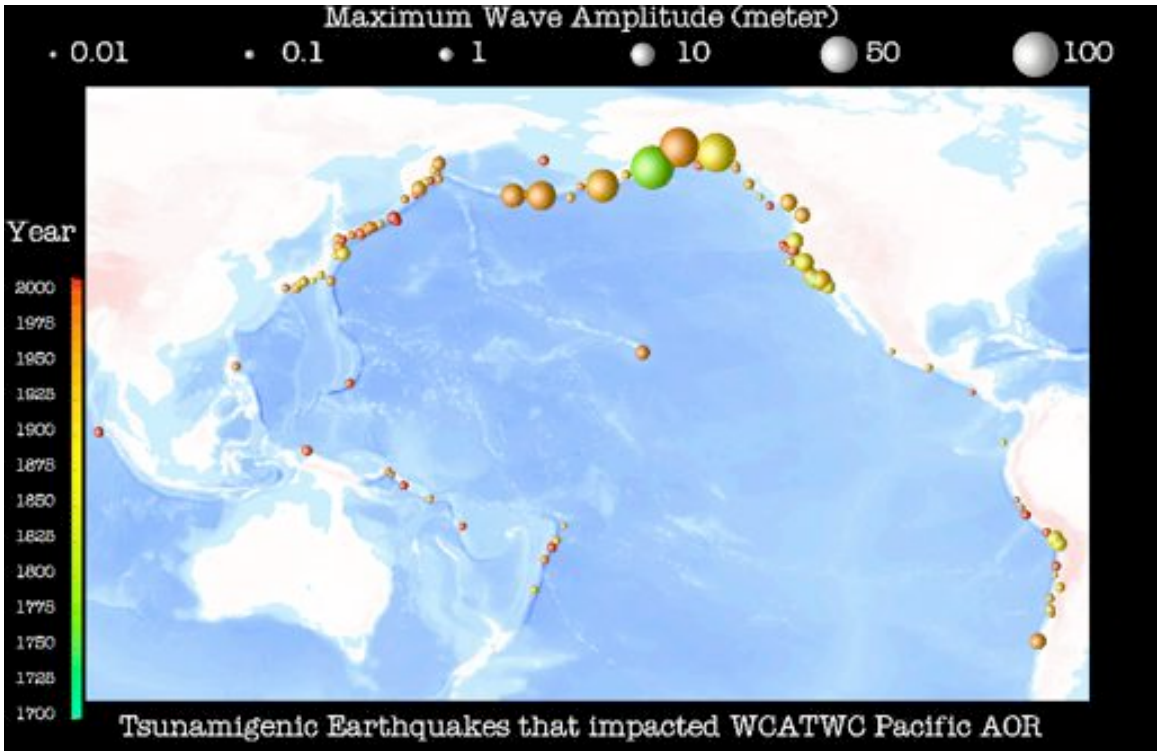

Figure 5. Events which have produced tsunamis recorded in the WCATWC Pacific AOR (NGDC, 2007). Spheres are located at the event's source location with a size related to the maximum recorded amplitude or runup within the AOR. The sphere color relates to the event's year of occurrence.

There are some pitfalls in using modeling to base criteria for local events. Most sub-sea earthquakes less than or near magnitude 7.5 do not trigger significant tsunamis. However, occasionally a major tsunami will be triggered by an earthquake in this range (e.g., 1998 Papua New Guinea, 1994 Java, and 2006 Java, etc). For these events, models computed using the expected sea floor displacement will normally show a non-dangerous wave about an order of magnitude less in size than the actual wave produced. The larger waves have been attributed to many phenomena, such as associated landslides, slow slip, and slip on splay faults through the accretionary wedge (e.g., associated landslides - Tappin *et al*. 2001; slow slip – Kanamori and Kikuchi 1993; slip through accretionary wedge – Fukao 1977).

Regardless of the reason for these larger than expected waves, criteria for local events can not be set only by forward modeling from earthquake sources. Criteria must be set conservatively enough so that the odds of a dangerous local event not falling within the warning category are very low.

Several earthquake source characteristics influence whether a tsunami is generated by an earthquake

and how large an area it may affect. The most obvious is earthquake size, or magnitude. Earthquake size can also be estimated by other features such as fault length, width, or slip. These other parameters are not known to the center analysts within the time frame necessary to issue the first message. There is little time for analysis during that first message output, so criteria must be kept as simple as reasonably possible.

Other earthquake source factors which can influence the likelihood of tsunami generation are earthquake location (onshore distance, relationship to tectonic features, and depth of water at epicenter), hypocentral depth, and the earthquake fault mechanism. All of these characteristics can influence how large an area can be affected by a wave if one is generated.

The influence of earthquake source parameters on tsunami generation is examined using the NGDC tsunami database. Table 2 compares hypocentral depth versus tsunami generation. Large, deep earthquakes are unusual in the AOR, so there is not much historical data for the AOR only. Table 2 includes all tsunamis throughout the entire planet since 1900 with amplitude 0.5m or over, and shows the percentage of occurrence at different hypocentral depth ranges.

Hypocentral Depth (km)	Number Tsunamis (entire database since 1900)	% of total tsunamis	Total # of earthquakes since 1900; M >= 7
< 50	343	90%	1300
50-100	35	9%	140
> 100	2	<1%	70

Table 2. Tsunami generation versus depth. Tsunamis included are all high-validity events worldwide since 1900 with amplitude greater than 0.5m. The last column shows the estimated total number of events over magnitude 7 for each depth range in this time period based on an extrapolation of the USGS Preliminary Determination of Epicenters catalog (2007).

Table 2 shows that the likelihood of tsunami generation by earthquakes greater than 100km depth is very low. However, earthquakes in the range 50km to 100km produce a sizeable portion of significant tsunamis. Results from this table support the international tsunami standard of not issuing tsunami warnings for earthquakes over 100km in depth except in cases where the size, depth, and location of the quake indicate possible rupture to shallow depths.

Table 3 compares earthquake magnitude with tsunami generation. Magnitudes are grouped by existing WCATWC criteria levels which match international standards.

Magnitude	Total number of earthquakes (U.S. west coast, BC, and Alaska) in potential tsunami generation areas (1900-2004)	Number of events which produced a tsunami >= 0.5m amp.	Maximum amplitude (m)	Maximum "reach" – max. epicentral distance with recorded amp. >= 0.5m (km)	Percentage of occurrence
5.0-5.9	3549	1	3	16	0.028%
6.0-6.4	422	0			0%
6.5-7.0	266	2	2.2	28	0.75%
7.1-7.5	55	3	3	146	5.5%
7.6-7.8	10	2	1+	870	20%
7.9+	13	7	525	Tele-tsunamis	59%

Table 3. Tsunami generation versus magnitude within the WCATWC AOR. Earthquakes of all depths are included in this table. Note: Three earthquakes M > 8.5 have occurred in the region since 1900 and all three triggered basin-wide tsunamis.

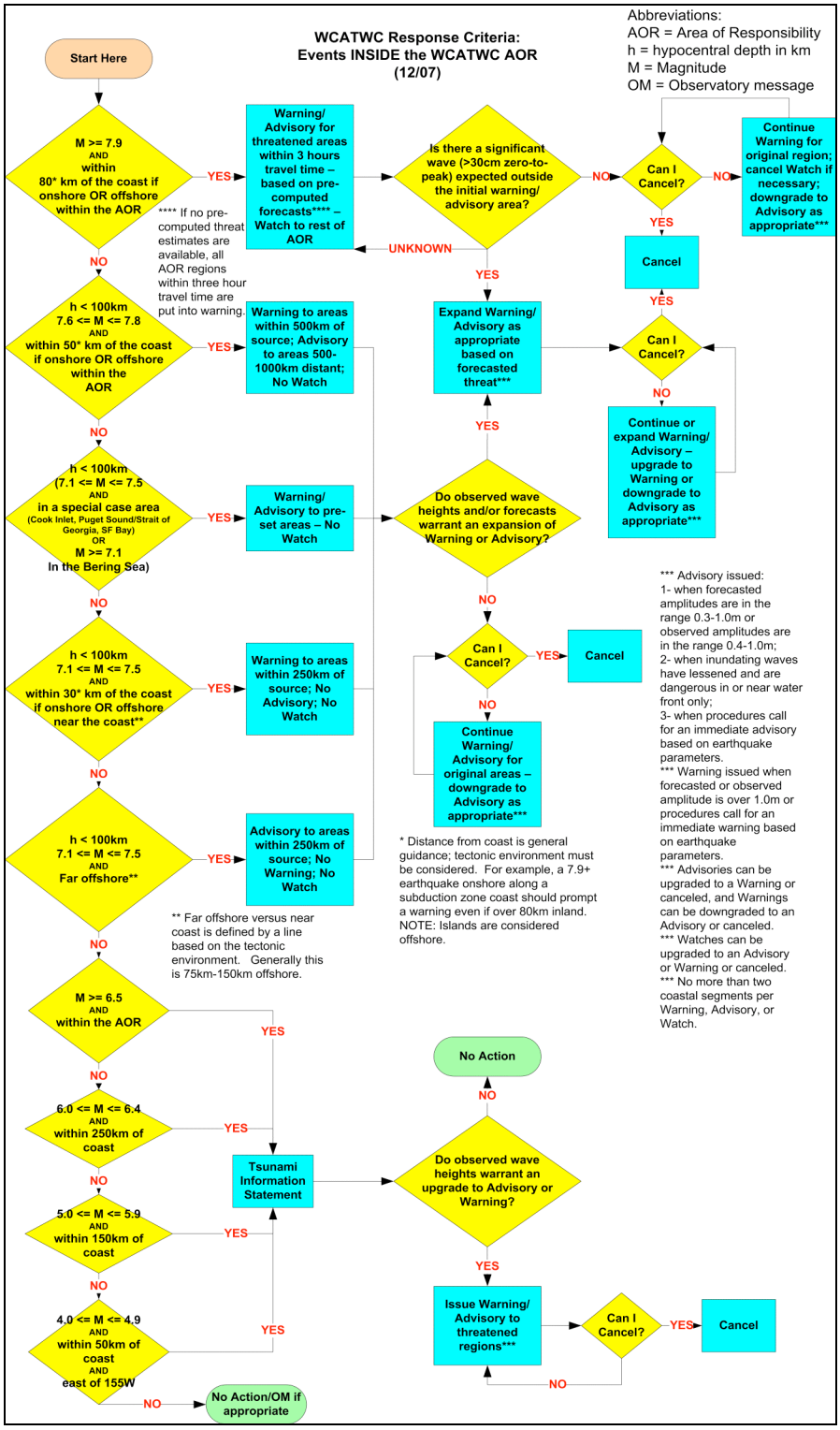

Figure 6. Warning criteria for events inside the WCATWC AOR.

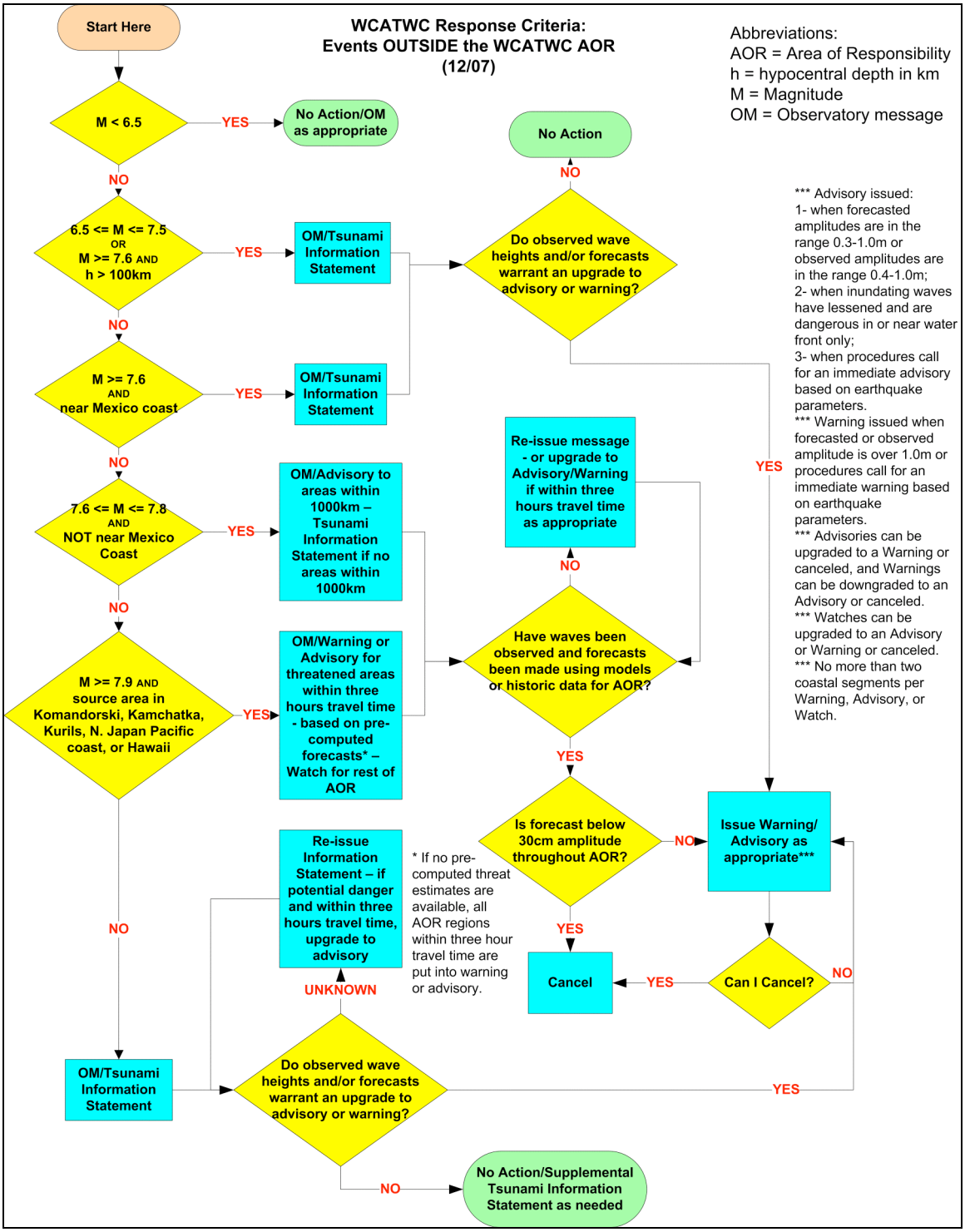

Figure 7. Warning criteria for events outside the WCATWC AOR.

Data in Table 3 show the general trend that the higher the earthquake magnitude, the more likely a tsunami will be generated. Also, the higher the magnitude, the further away from the epicenter the wave may be dangerous. Data on this table support keeping warning zones small for events magnitude 7.5 and below, and increasing the geographic extent with magnitude. WCATWC response criteria corresponding to the magnitude ranges given in Table 3 are shown in the flow charts in Figures 6 and 7.

Earthquake fault mechanism also influences tsunami generation. Intuitively, it might seem that events with horizontal fault motion should not produce tsunamis as little sea floor is vertically moved. However, Knight (2006) and Geist and Parsons (2005) showed that earthquakes with horizontal fault motion can produce significant tsunamis. Potential generation mechanisms include triggering of sub-aerial or sub-marine landslides, horizontal motion of an inclined sea floor, and slip vector obliqueness. Table 4 summarizes strike-slip events which produced large tsunamis from 1977 to 2004. Fault parameters are taken from the Global Centroid Moment Tensor Project Database (2007). Of the nearly 4000 earthquakes listed in the database, 109 produced a tsunami and 41 of those produced tsunamis greater than 1m amplitude. Of those 41 events, 5 (12%) were triggered by strike slip earthquakes (with slip vectors within 20 degrees of horizontal).

Event Date	Region	Magnitude	Maximum amplitude (m)	"Reach" – max. epicentral distance with recorded amp. >= 0.5m (km)	Notes
9/12/1979	Irian Jaya	7.5	2.0	75	
1/21/1994	Indonesia	6.9	2.0	30	
10/8/1994	Indonesia	6.8	3.0	10	1 death
11/14/1994	Philippines	7.1	7.2	35	24 deaths
10/10/2002	Irian Jaya	7.5	4.0	75	Flooding

Table 4. Strike slip earthquakes which produced significant tsunamis in the period from 1977 to 2004 (Knight, 2006).

Table 4 shows that strike slip events can cause tsunamis, though, all of these earthquakes were located near the coast. In each case, the event was located within 25km of the coastline the tsunami impacted.

Based on the information given in Tables 3 and 4 and the high likelihood of strike slip events occurring far offshore the Pacific Northwest coastline, events in the magnitude range 7.1-7.5 and located far offshore will trigger the issuance of an advisory for nearby coasts. Those located near shore will trigger the issuance of a warning. The definition of zones which trigger warning versus advisory in the 7.1 to 7.5 magnitude range is defined by an examination of the tectonic environment, and is normally based on distance ocean-ward from the trench. Figure 8 shows the warning/advisory boundary for the Cascadia subduction zone region.

An interesting strike slip event not shown on Table 4 which occurred in the WCATWC AOR is the 1987, M=7.8, Gulf of Alaska event. This event triggered an observable wave in Yakutat, Alaska of 0.4m amplitude. The event occurred well onto the oceanic plate, far from any inclined features or slopes expected to slide, but still produced a near-dangerous-amplitude wave. Based on the

procedures listed in Figure 6, a warning would be issued for this event to areas within 500km and an advisory to areas from 500km to 1000km distant. Appendix A shows the distribution of warning/watch/advisory areas for this event and other historic events using both the criteria listed in this report and criteria used at the time of the event.

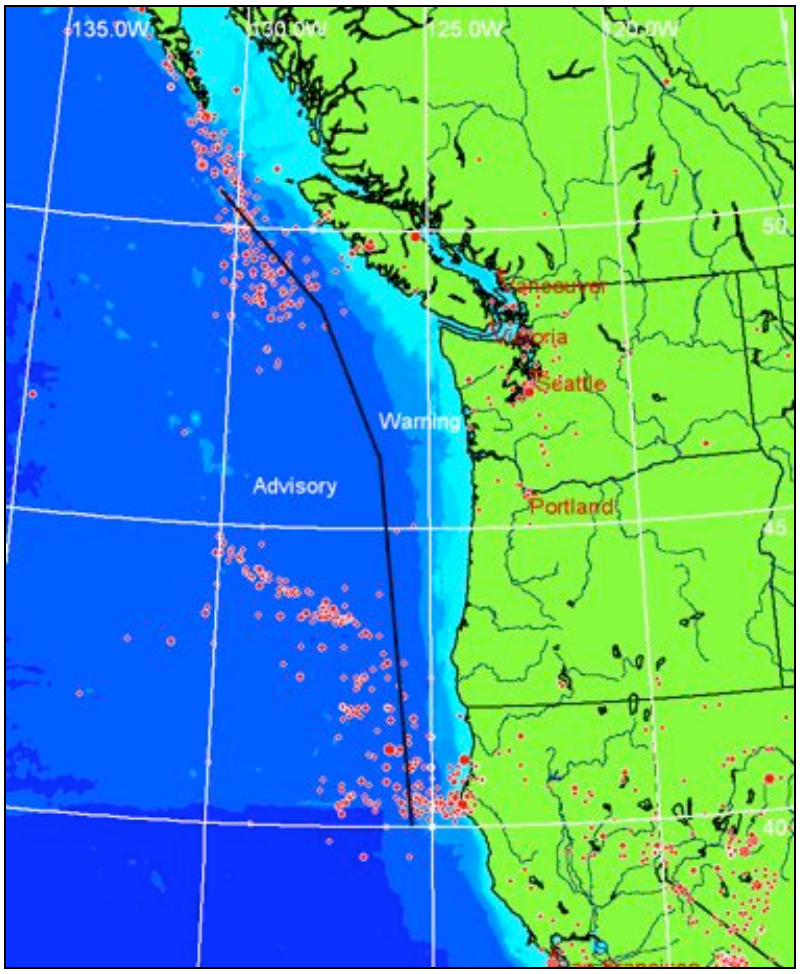

Figure 8. Line dividing offshore magnitude 7.1 to 7.5 earthquakes (which trigger advisories) from near shore earthquakes (which generate warnings) in the Cascadia subduction zone region. Historic earthquakes are shown with red dots.

Criteria relating to epicentral distance from the coast for on-shore events are also provided in Figure 6. The distances vary with magnitude and are relevant for epicenters located on the North American mainland. Epicenters located on islands such as Kodiak and Vancouver are treated as offshore events.

There are a few examples of on-shore events which have produced tsunamis. The two main reasons that an on-shore event can trigger a tsunami are: 1) the fault rupture extends under the ocean (e.g., 1964 Alaska quake and 1906 San Francisco quake), and 2) strong shaking induces a sub-aerial or sub-marine landslide (e.g., 1989 Loma Prieta).

Table 5 summarizes on-shore events in the AOR which have triggered tsunamis. Since 1900, 37 known tsunamis have been generated in the AOR. Seven of these were generated by events with an epicenter on land.

Table 5. Onshore events in the WCATWC AOR which have triggered a tsunami (NGDC, 2007).

Event Date	Region	Magnitude	Maximum amplitude (m)	Epicentral distance from coast (km)	Cause
6/23/1946	Vancouver I.	7.3	3 (?)	10	Landslide
4/13/1949	Washington	7.0	2.2	2	Landslide
7/10/1958	Alaska	8.2	525	1	Landslide
3/28/1964	Alaska	9.2	67	2	Extended fault rupture and landslides
2/28/1979	Alaska	7.4	0.1	65	Ice fall (?)
10/18/1989	California	6.9	1	3	Landslide
4/25/1992	California	7.2	0.9	4	Extended fault rupture

The events in Table 5 indicate that sources have to be near the coast to trigger a tsunami. The 1964 event is a little misleading, though. It was located within 2km of the ocean, but next to a fjord which extended well into the mainland. The fault rupture (and tsunami source zone) extended several hundred kilometers seaward from the epicenter.

The distance an earthquake ruptures is roughly related to its magnitude. Several studies have developed rupture length versus magnitude relationships. All these relationships are best fits to the observed data and do not provide an accurate estimate for all events. Papazachos, et al. (2004) separated the relationship into strike slip, continental dip slip, and subduction dip slip categories. Table 6 summarizes expected fault length for these categories. These values could be used as guidelines as they would limit how far an event could be from the coast and still directly disturb the sea floor (if the hypocenter is located near one end of a rupture zone).

Table 6. Expected rupture length for various size earthquakes and tectonic settings (Papazachos et al., 2004).

Magnitude	Fault Type	Expected Rupture Length (km)
7.0	Strike Slip	67
7.0	Continental Dip Slip	44
7.0	Subduction Zone Dip Slip	46
7.5	Strike Slip	133
7.5	Continental Dip Slip	78
7.5	Subduction Zone Dip Slip	86
7.8	Strike Slip	200
7.8	Continental Dip Slip	110
7.8	Subduction Zone Dip Slip	126
8.0	Strike Slip	263
8.0	Continental Dip Slip	138
8.0	Subduction Zone Dip Slip	162

Tables 5 and 6 provide much different sets of guidelines for onshore earthquake criteria. Using the fault lengths in Table 6 as a guide would lead to over-warning based on the history shown in Table 5. Another factor which could help a TWC analyst in certain cases is the ShakeMaps produced by the Advanced National Seismic System (ANSS). For many areas of the United States, ShakeMaps are quickly distributed by the ANSS and available at the WCATWC shortly after initial bulletin issuance. Further work is necessary to integrate ShakeMaps fully into tsunami warning center operations.

Onshore distance guidelines are set conservatively based on the history in Table 5. Following initial message issuance, the analyst would attempt to verify that fault rupture has not extended to sea by using the ShakeMap, fault mechanism, and/or nearby sea level data (upgrading the message if necessary). As specified in the Figure 6 flowchart, one exception to the distance rule is major (magnitude 7.9+) onshore earthquakes in a subduction zone. These will prompt a warning even if the hypocenter is greater than the set distance from the coast.

Based on the discussion above and information in Tables 2 through 6, warning criteria for events inside and outside the WCATWC AOR are given in a flowchart form in Figures 6 and 7. These criteria have several differences from the previous criteria used at the center:

- Hypocentral depth is included,
- Geographical warning extent is generally reduced,
- Special procedures are set for regions not well-connected to the open ocean,
- For events magnitude 7.9+, warning/advisory areas are based on threat level from pre-computed models instead of tsunami travel times,
- The new advisory product is included in the criteria,
- Advisories are issued for far-offshore events in the lower magnitude ranges, and
- For onshore events, distance from the coast is specified.

Operationally, basing the warning extent on modeled threat level versus tsunami travel times for events magnitude 7.9 and greater is a significant change. Recent improvements in modeling and sea level data acquisition make this change possible. The new DART array provides data to the TWC which allows the center to forecast impact for distant events well before wave impact along the AOR coast. The new criteria take advantage of this array by only issuing immediate warnings/advisories to areas that could be affected within three hours of the event. Within this three-hour region, only areas that pre-computed tsunami models indicate will be threatened are put into a warning or advisory. If no threat analysis is available for a source, warnings/advisories will be issued to all AOR coasts within three hours travel time until recorded sea level data allows cancellation or restriction of the warning/advisory.

Threatened areas are defined by using tsunami models (Titov and Gonzalez 1997, Whitmore and Sokolowski 1996). Models are computed for different magnitude events at subduction zones around the Pacific basin which could threaten the AOR. Based on the amplitudes computed, the region of the AOR threatened in each model is defined. During an event, the most appropriate model is selected and its threatened area is compared with travel times to determine the region placed in a warning or advisory.

For example, during the November 15, 2006 Kuril Islands event, warnings were issued for regions of the Aleutian Islands within three hours of the wave front until a forecast could be made (based on procedures of the time). Areas east to Sand Point, AK were eventually included in warnings. Pre-computed, unscaled models forecasted minor waves (0.12m and less) east of Adak in Alaska, and moderate waves (0.2m to 0.4m) from Adak west to Attu. Under the new procedures, the region from Adak to Attu would have been issued an immediate advisory which would not have expanded to the east unless observed wave heights indicated otherwise (Figure A4). The region from Adak to Attu was the only region in Alaska that models forecasted an advisory level impact (0.3m to 1.0m). Warnings and advisories for areas along the west coast would be based on a forecast calibrated with observed sea level heights.

Warning, watch, and advisory areas are delineated by known break points. These break points are listed below.

Attu, AK	Yakutat, AK	Cape Blanco, OR
Adak, AK	Sitka, AK	Oregon-California Border
Nikolski, AK	Langara Island, BC	Cape Mendocino, CA
Dutch Harbor, AK	Northern Tip Vancouver Island, BC	Point Reyes, CA
Sand Point, AK	Washington-BC Border	Point Sur, CA
Kodiak, AK	Clatsop Spit, OR	Point Conception, CA
Seward, AK	Cascade Head, OR	California-Mexico Border
Cordova, AK		

The flow chart in Figure 6 lists four areas which have special procedures (Bering Sea, Cook Inlet, Puget Sound/Strait of Georgia, and San Francisco Bay). Figure 9 depicts the Puget Sound special procedure area. Tsunamis generated in these areas are expected to be confined to the source region only. Warning zones are pre-determined for events that occur within the specified region and magnitude range. These zones are based on a study of potential sources and wave propagation for each region. For example, a magnitude 7.1 or greater earthquake located east of Russia in the Bering Sea would prompt a warning for the Pribilof Islands, and the Aleutian Islands from False Pass to Attu. Another example is the Puget Sound special procedural region for earthquakes in the magnitude range 7.1 to 7.5 (Figure 9). Earthquakes within this magnitude range and region would prompt a warning for the Puget Sound and Strait of Juan de Fuca and not the outer coast.

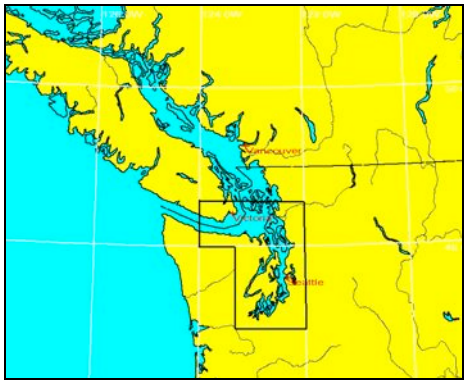

Figure 9. Puget Sound special procedure region.

The seismic-based criteria given on the left sides of Figures 6 and 7 are for initial message issuance. Supplemental messages can be further guided by fault mechanism analysis, ANSS ShakeMaps, and slow earthquake discrimination by energy versus moment comparisons if sea level data and associated forecasts are not available.

6. FUTURE WORK

Warning criteria refinement is an ongoing process. Continued collaboration between warning centers, research agencies, and emergency management through channels such as the U.S. National Tsunami Hazard Mitigation Program (Bernard 2005) are necessary to keep criteria up-to-date with the latest knowledge and emergency management response capabilities. New observational data sets, processing techniques, and basic hazard research must be incorporated into the criteria as they become available. Some ideas to address are:

- Utilize USGS ShakeMap and mechanism products and slope stability analysis to determine areas at highest risk of landslide tsunami generation,
- Improve near source tsunami observations and corresponding forecast models,
- Incorporate real time GPS/accelerometer data streams to improve finite fault parameter determinations, and
- Investigate seismic techniques which help discriminate earthquakes likely to generate a tsunami from those that are not.

7. ACKNOWLEDGEMENTS

The authors thank Paul Bodin and John Vidale of the University of Washington for contributions to the report, and to Paul Huang, Bill Knight, and Cindi Preller of the WCATWC for assistance with graphics and historical data mining.

8. REFERENCES

Bernard, E. N., 2005. The U.S. National Tsunami Hazard Mitigation Program: A successful state-federal partnership, *Natural Hazards*, **35**, 5-24.

Fukao, Y., 1979. Tsunami earthquakes and subduction processes near deep-sea trenches, *J. Geophys. Res*., **84**, 2303-2314.

Geist, E. and T. Parsons. 2005. Triggering of tsunamigenic aftershocks from large strike-slip earthquakes: Analysis of the November 2000 New Ireland earthquake sequence. *Geochemistry, Geophysics, Geosystems 6(10): doi: 10.1029/2005GC000935. issn: 1525-2027.*

Global Centroid Moment Tensor Project Database. 2007. http://www.globalcmt.org/CMTsearch.html.

Kanamori, H. and M. Kikuchi, 1993. The 1992 Nicaragua earthquake: a slow tsunami earthquake associated with subducted sediments, *Nature*, **361**, 714-716.

Knight, W. 2006. Strike Slip Tsunami Sources. Abstract, The Tsunami Society Third Tsunami Symposium, Honolulu, Hawaii.

Knight, W. 2006. Model predictions of Gulf and southern Atlantic coast tsunami impacts from a distribution of sources, *Sci. Tsu. Hazards,* **24**, 304-312.
Lander, J., P. A. Lockridge and J. Kozuch. 1993. Tsunamis affecting the west coast of the United States 1806-1992, NGDC Key to Geophysical Research Documentation No. 29, USDOC/NOAA/NESDIS/NGDC, Boulder, CO, USA, 242 pp.
Lander, J. 1996. Tsunamis affecting Alaska 1737-1996, NGDC Key to Geophysical Research Documentation No. 31, USDOC/NOAA/NESDIS/NGDC, Boulder, CO, USA, 195 pp.
National Geophysical Data Center Tsunami Database. 2007. Revised November 6, 2007. http://www.ngdc.noaa.gov/seg/hazard/tsu_db.shtml.
Papazachos, B.C., E.M. Scordilis, D.G. Panagiotopoulos, C.B. Papazachos, and G.F. Karakaisis. 2004. Global relations between seismic fault parameters and moment magnitude of earthquakes, *Bull. Geol. Soc. Of Greece,* **36,** 1482-1489.
Tappin, D. R., P. Watts, G. M. McMurty, Y. Lafoy, and T. Matsumoto, 2001. The Sissano, Papua New Guinea tsunami of July 1998 – offshore evidence on the source mechanism, *Marine Geology*, **175**, 1-23.
Tatehata, H., 1998. The new tsunami warning system of the Japan Meteorological Agency, *Sci. Tsu. Hazards,* **16**, 39-50.
Titov, V.V. and F.I. Gonzalez. 1997. Implementation and testing of the Method of Splitting Tsunami (MOST) model, NOAA Technical Memorandum ERL PMEL-112, 11 pp.
United States Geological Survey Earthquake Hazards Program Global Earthquake Data Base. 2007. Revised November 5, 2007. http://wwwneic.cr.usgs.gov/neis/epic/epic.html.
Whitmore, P. M. 2003. Tsunami amplitude prediction during events: a test based on previous tsunamis, *Sci. Tsu. Hazards,* **21**, 135-143.
Whitmore, P. M. and T. J. Sokolowski. 1996. Predicting tsunami amplitudes along the North American coast from tsunamis generated in the northwest Pacific Ocean during tsunami warnings, *Sci. Tsu. Hazards,* **14**, 147-166.

APPENDIX A

Four examples are provided below which show the initial warning/ watch/ advisory status for historic events. Both the status using criteria in use at the time of the event and the criteria given in this report are shown.

Example 1:
1987 M=7.8 Gulf of Alaska

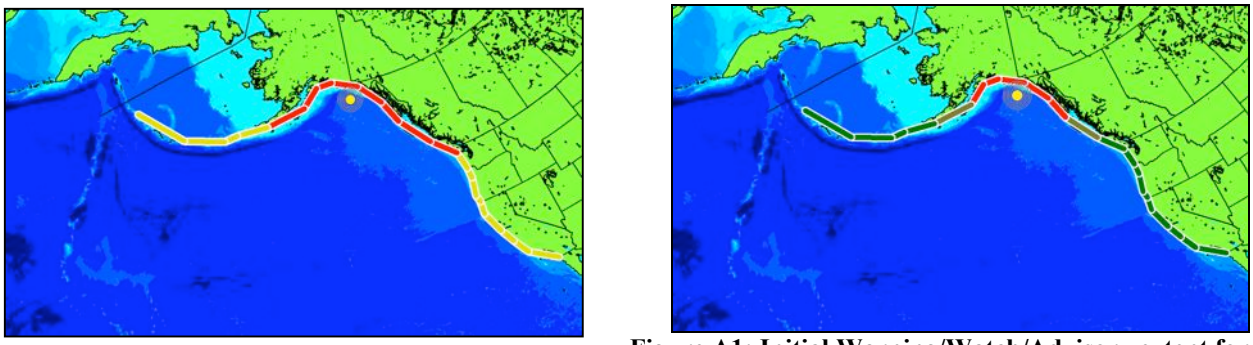

Figure A1: Initial Warning/Watch/Advisory extent for the 1987 Gulf of Alaska event. The left side shows the actual extent of the initial alert and the right shows the extent under the criteria listed in this report. Warning areas in red; advisory in grey, watch in yellow; information only in green.

Example 2:
1997 M=7.8 Kamchatka

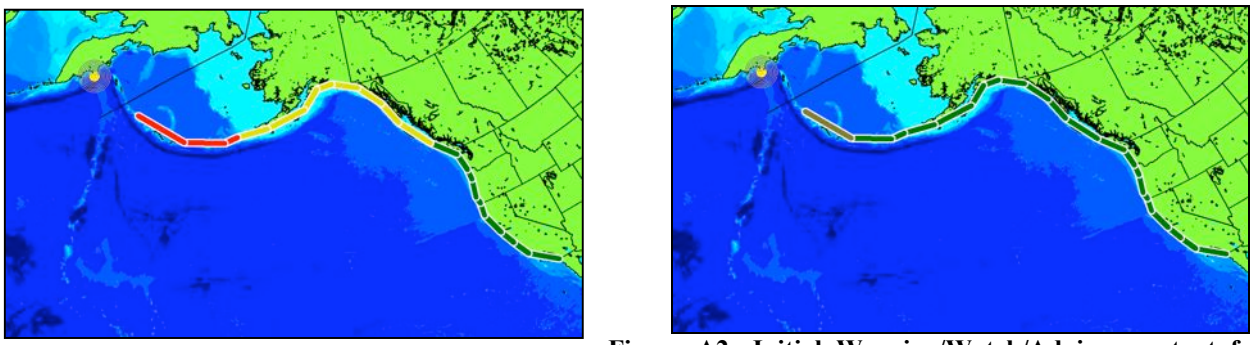

Figure A2: Initial Warning/Watch/Advisory extent for the 1997 Kamchatka event. The left side shows the actual extent of the initial alert and the right shows the extent under the criteria listed in this report. Warning areas in red; advisory in grey, watch in yellow; information only in green.

Example 3:

2005 M=7.2 Gorda Plate

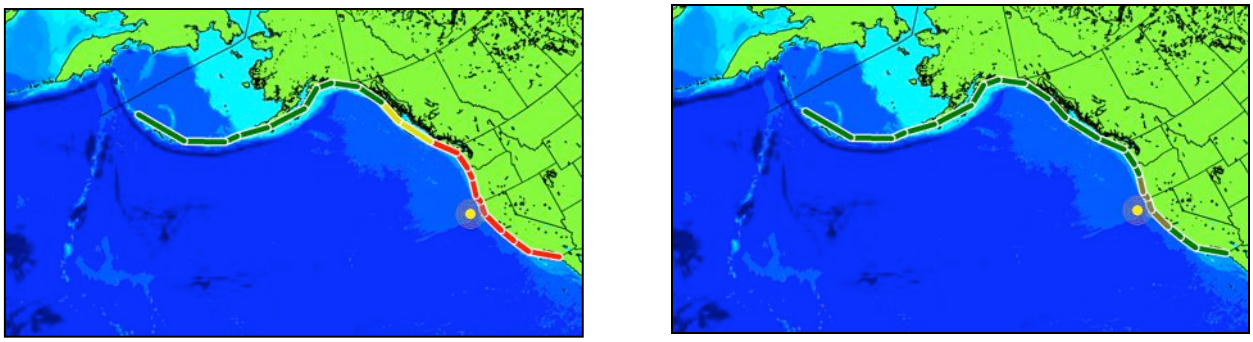

Figure A3: Initial Warning/Watch/Advisory extent for the 2005 Gorda plate event. The left side shows the actual extent of the initial alert and the right shows the extent under the criteria listed in this report. Warning areas in red; advisory in grey, watch in yellow; information only in green.

Example 4:

2006 M=8.3 Kuril Islands

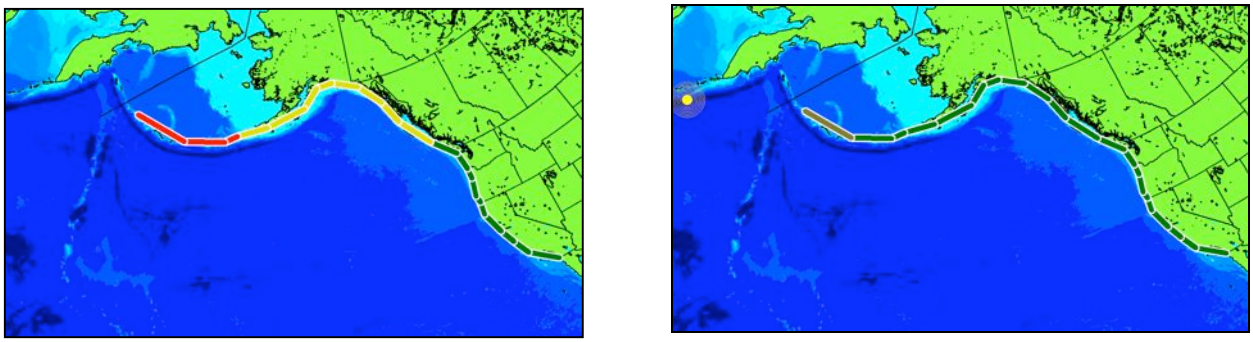

Figure A4: Initial Warning/Watch/Advisory extent for the 2006 Kuril Islands event. The left side shows the actual extent of the initial alert and the right shows the extent under the criteria listed in this report. Warning areas in red; advisory in grey, watch in yellow; information only in green.

DID A SUBMARINE SLIDE TRIGGER THE 1918 PUERTO RICO TSUNAMI?

Matthew J. Hornbach[1], Steven A. Mondziel[2], Nancy R. Grindlay[2], Cliff Frohlich[1], Paul Mann[1]

For submission to *Science of Tsunami Hazards*

Corresponding author: Matthew J. Hornbach
matth@ig.utexas.edu

[1] The Institute for Geophysics, The Jackson School of Geosciences, The University of Texas at Austin, Austin, Texas, USA.

[2] University of North Carolina at Wilmington, Department of Geography and Geology. Wilmington, North Carolina, USA.

ABSTRACT

The 1918 tsunami that inundated northwest Puerto Rico with up to 6 m waves has been attributed to seafloor faulting associated with the 1918 Mona Canyon earthquake. During the earthquake a series of submarine cable breaks occurred directly off the northwest coast of Puerto Rico where the largest tsunami waves came ashore. Here, we use a recently compiled geophysical data set to reveal that a 9 km long landslide headwall exists in the region where cable breaks occurred during the 1918 earthquake. We incorporate our interpretations into a near-field tsunami wave model to evaluate whether the slide may have triggered the observed 1918 tsunami. Our analysis indicates that this slide could generate a tsunami with phase, arrival times, and run-ups similar to observations along the northwest coast of Puerto Rico. We therefore suggest that a submarine slide offers a plausible alternative explanation for generation of this large tsunami.

Introduction

Although tsunamis immediately following large earthquakes are routinely attributed to earthquake-induced seafloor faulting, submarine slides, which sometimes accompany large earthquakes, can produce destructive tsunamis [*Heinrich et al.*, 2001; *Tappin et al.*, 1999; *Tinti et al.*, 1999]. Both earthquakes and submarine slides generate tsunamis by displacing water during seafloor deformation, however, for any particular scenario of seafloor deformation (i. e., timing, source location, size, direction of motion) the resulting wave is unique [eg. *Heinrich et al., 2000; Ioualalen et al., 2006*]. By analyzing bathymetric data and earthquake fault mechanisms in tsunamigenic regions, one can constrain seafloor deformation patterns, forward-model the resulting near-field tsunamis, and identify the deformation pattern that best reproduces the observed wave.

The 1918 Puerto Rico tsunami is one of the first modern tsunami events where high-quality observations of tsunami wave phase, run-up, and arrival times were well documented, allowing for good comparison with tsunami wave models [*Mercado and McCann*, 1998; *Reid and Taber*, 1919]. Previous studies [*Mercado and McCann*, 1998] suggest that seafloor deformation caused by fault rupture of the 11 October 1918 Mw 7.3 Puerto Rico earthquake [*Engdahl and Villase–or*, 2002] generated the tsunami with wave run-up as high as 6 m along the northwest coast, that killed more than 100 people [*Reid and Taber*, 1919]. Re-analysis of the 1918 earthquake epicenter indicates that although significant (+/- 50 km) uncertainty in its exact location exists, the predicted epicenter is consistent with proposed faults that triggered the tsunami [*Doser et al.*, 2005; *Mercado and McCann*, 1998]. Analysis also indicates that the event was not a slow "tsunami earthquake," where earthquake moment magnitude is significantly larger than surface magnitude and uncharacteristically long and slow rupturing occurs [*Doser et al.*, 2005; *Kanamori and Masayuki*, 1993]. Nonetheless, surprisingly high (2-6 m) wave run-ups occurred along a localized, 15-20-km-long coastal segment of northwestern Puerto Rico between Pt. Boqueron and Pt. Higuero [*Reid and Taber*, 1919] (Figure 1).

Perhaps more importantly, however, independent evidence exists that the earthquake caused a submarine slide. Specifically, during the earthquake, multiple submarine cable breaks occurred to the northwest of Puerto Rico, just north of the epicenter [*Reid and Taber*, 1919] (Figure 1A). Cable breaks are commonly associated with submarine slides [e.g. *Krause et al.,*1970]. To date, there is no detailed bathymetric study confirming that a submarine slide occurred in this area. Here, by combining results from recently merged high-resolution seismic and bathymetric data, historical records, and a near-field tsunami model, we assess the plausibility that a submarine slide triggered the large 1918 tsunami observed along northwest coast of Puerto Rico. Using seismic and bathymetric data, we show that a large headwall exists within the cable break region, north of the Mona Canyon, and we suggest that a slide from this headwall caused the cable breaks during the 1918 earthquake and a may have triggered the tsunami.

Imaging Methods

We compiled multibeam bathymetry data from six research cruises performed over the period 1995-2004 in the northeast Mona Passage in the region of the suspected origin of the 1918 tsunami. These data sets include Atlas Hydrosweep and Seabeam 2112 multibeam bathymetry data. Recent coastal relief measurements from the northeast Mona Passage supplied by NOAA's online National

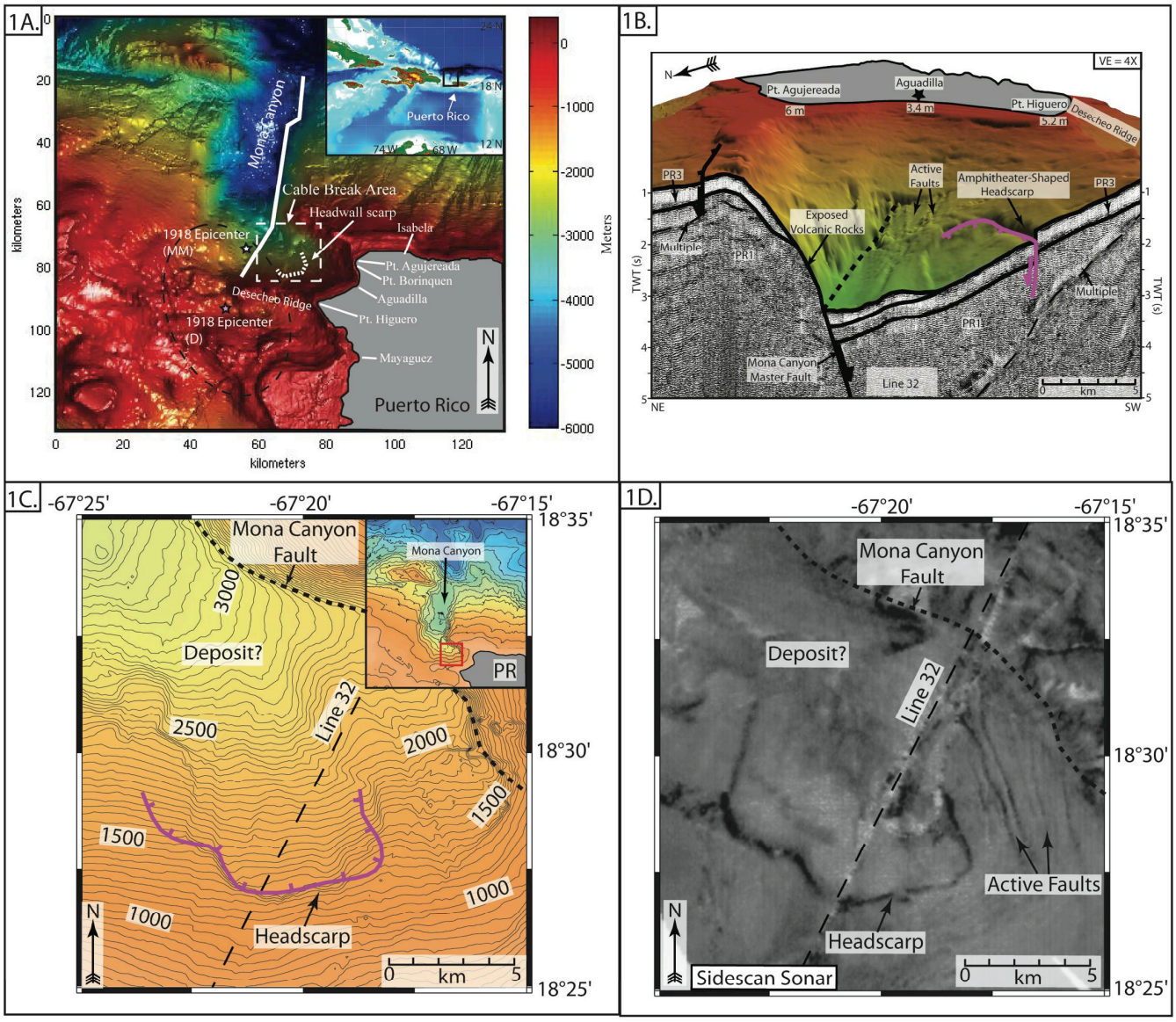

Figure 1. (A) 150 m resolution bathymetric map created from interpolating multibeam data collected along the northwest coast of Puerto Rico (inset shows regional location). The revised earthquake epicenter is south of the Mona Canyon. The dashed ellipse represents the new location of the 1918 earthquake epicenter (centered at the pink star) with 90% confidence [*Doser et al.*, 2005]. The white star represents the approximate location of the 1918 epicenter, according to *Pacheco and Sykes* [1992]. The solid white line shows the approximate location of proposed faults that may have slipped during the 1918 earthquake, suggested by *Mercado and McCann* [1998]. The dashed white box indicates the region where cable breaks occurred according to *Reid and Taber* [1919]. (B) Oblique view of seafloor and seismic line 32, collected across the cable break region and the newly discovered headscarp (pink). (C) Bathymetric data in the vicinity of the headscarp and cable break zone. (D) Sidescan sonar of the same area in (C).

Geophysical Database Center (NGDC) supplement these multibeam bathymetry data sets. All multibeam bathymetry data were processed and merged to generate a digital terrain model (DTM) of all data sets at a 150-m grid interval. We also included sidescan sonar imagery collected with the Hawaii Mapping Research (HMR) group's HMR-1 sidescan sonar system as part of research cruise EW9605. The data were slant-range and beam-angle corrected and gridded at a 17m interval. Single-channel seismic reflection data collected aboard research cruise EW9605 in the northeast Mona Passage in the suspected source region of the 1918 tsunami were processed through migration using Parallel Geoscience's Seismic Processing Workshop (SPW). We combined these data with the multibeam bathymetry and sidescan sonar data to generate pseudo three-dimensional images of the seafloor. We analyzed these data, searching for breaks in the surficial sediments indicating potential active faults, and for amphitheatre-shaped headscarps indicating the presence of submarine landslides.

Imaging Results

Multiple mass wasting features are evident in the Mona Canyon in the multibeam bathymetry, sidescan sonar, and seismic reflection data [*Grindlay et al.*, 2005; *ten Brink et al.*, 2006]. Of particular interest is a nearly semi-circular headscarp centered at 18.46^{o} north, -67.33^{o} west at ~1200 m water depth that extends ~9 kilometers northeast-to-southwest, with an average height of ~100 m, and a maximum height of ~200 m (Figure 1). This feature is approximately 18 km off the northwest coast of Aguadilla, Puerto Rico and is located in the same region as two submarine cable breaks documented by *Reid and Taber* [1919]. However, because the available seismic sections are widely spaced the exact limits of the downslope slide deposit remain poorly known. From the shape and length of the headwall (a semi-circular feature approximately ~9 km long and ~100 m high), we estimate that the maximum slide volume, assuming this was a single contiguous slide event, is no greater than ~6 km^{3}.

We propose that the 11 October 1918 M_{W} 7.3 earthquake re-activated motion along the antithetic (east-dipping) fault on the hanging wall of the southern Mona Canyon half-graben (north of Desecheo Ridge) (Figure 1B). We proposed that seafloor rupture of this fault triggered a slope failure that subsequently broke the submarine cables as it traversed down slope, displaced the water column, and generated the 2-6 m-high tsunami that inundated the northwest coast of Puerto Rico.

Comparison of Imaging Results with Historic Observations

Our observations are in excellent agreement with more limited observations made by ocean bottom cable surveyors, who studied the bathymetry in the cable-break region immediately following the earthquake. Specifically, the captain of the cable repair ship noted that depth soundings obtained during cable repair indicated an apparent increase in depth of as much as183 meters in the cable break area, although relatively poor navigation might also explain this discrepancy [*Reid and Taber*, 1919]. Perhaps more revealing, however, is that the cable repair crew found long sections ("two-to-three miles") of cable crushed and buried underneath sediment in this region [*Reid and Taber*, 1919]. The correlation of the bathymetric study results with the cable repair observations strongly suggest that a kilometer-scale submarine slide occurred in this vicinity during the 1918 earthquake.

Submarine Slide Modeling

We used seafloor bathymetric data combined with previously published submarine slide models to estimate slide motion. The bathymetric data fix the location of the headwall and the slope of the seafloor, and we use these parameters to constrain slide size, direction, and velocity. To estimate of slide size, we assume it had a maximum width and height of 9 and 0.2 km, respectively. These are maximum values, since it is possible that only a portion of the headwall failed, and that the headwall potentially formed piecemeal during multiple individual slide events. The length of the slide is difficult to determine, and would require a high resolution coring and seismic study to constrain fully. Given the roughly symmetric, scalloped-shaped headwall, we here assume a symmetric slide, and model it as a 2D Gaussian function with a diameter (2-sigma) of 9 km and a maximum height of 200 m, resulting in a maximum slide volume of ~6 km^3. As noted in previous tsunami modeling studies [*Ward*, 2001], an increase/decrease in slide volume will result in a corresponding increase/decrease in tsunami wave height. For a first-order model of slide motion, we assume the slide accelerates uniformly down-slope, consistent with submarine slide modeling and experiments [*Grilli and Watts*, 1999; *Watts*, 1997], and we also assume a seafloor slope of 7¡ a mean slide direction of ~305¡E of N, both estimated from bathymetric data. It remains unclear from the bathymetric data how far the slide transports material down slope and where break-up occurs; given that no clearly identifiable large slide blocks exist down slope with this event, we suggest that as the slide accelerated down slope, it gradually broke-up, dispersed, and distributed debris over a large area. Previous slide tsunami modeling studies show that slide deceleration and evolution have only second order effects on tsunami wave development [*Jiang and LeBlond*, 1992; *Watts et al.*, 2005], and we therefore assume that slide initiation generates the primary tsunami wave. Indirect measurements of slide velocities from the timing and location of cable breaks at other known slides indicate that the group velocity of slide material likely does not exceed 30-40 m/s [e.g. *Krause et al.,1970*], and therefore, we limit terminal slide velocity to 40 m/s.

Tsunami Modeling

We use a standard hydrostatic non-linear long wave model to characterize the tsunami generated by the submarine slide [eg. *Heinrich et al.*, 2000; *Tinti et al.*, 1999]. Because the tsunami source area is close (<25 km) to where the near-field wave impacts shore, the finite-difference code incorporates a non-dispersive leap-frog wave propagation technique to model the wave through time and incorporates both Coriolis and frictional forces. For bathymetry, we use the previously described bathymetric data collected from multibeam surveys, gridded at 150 m intervals, with a total model domain of 680 square cells.

The wave propagation model enables us to assess wave phase, arrival times, and wave run-up for the slide-generated near-field tsunami. Although far-field tsunami waves were recorded during this tsunami event (with the most distant wave detected via tide-gauges along the US east coast [*Reid and Taber*, 1919]), analysis of this far-field data requires a much larger high-resolution grid than we currently have, and such an analysis goes beyond the scope of the this data set, this model, and this study. Although near-field wave phase, arrival times, and run up can all be accurately determined using this tsunami model, wave run-up will have the greatest error due to (1) shoreline bathymetric

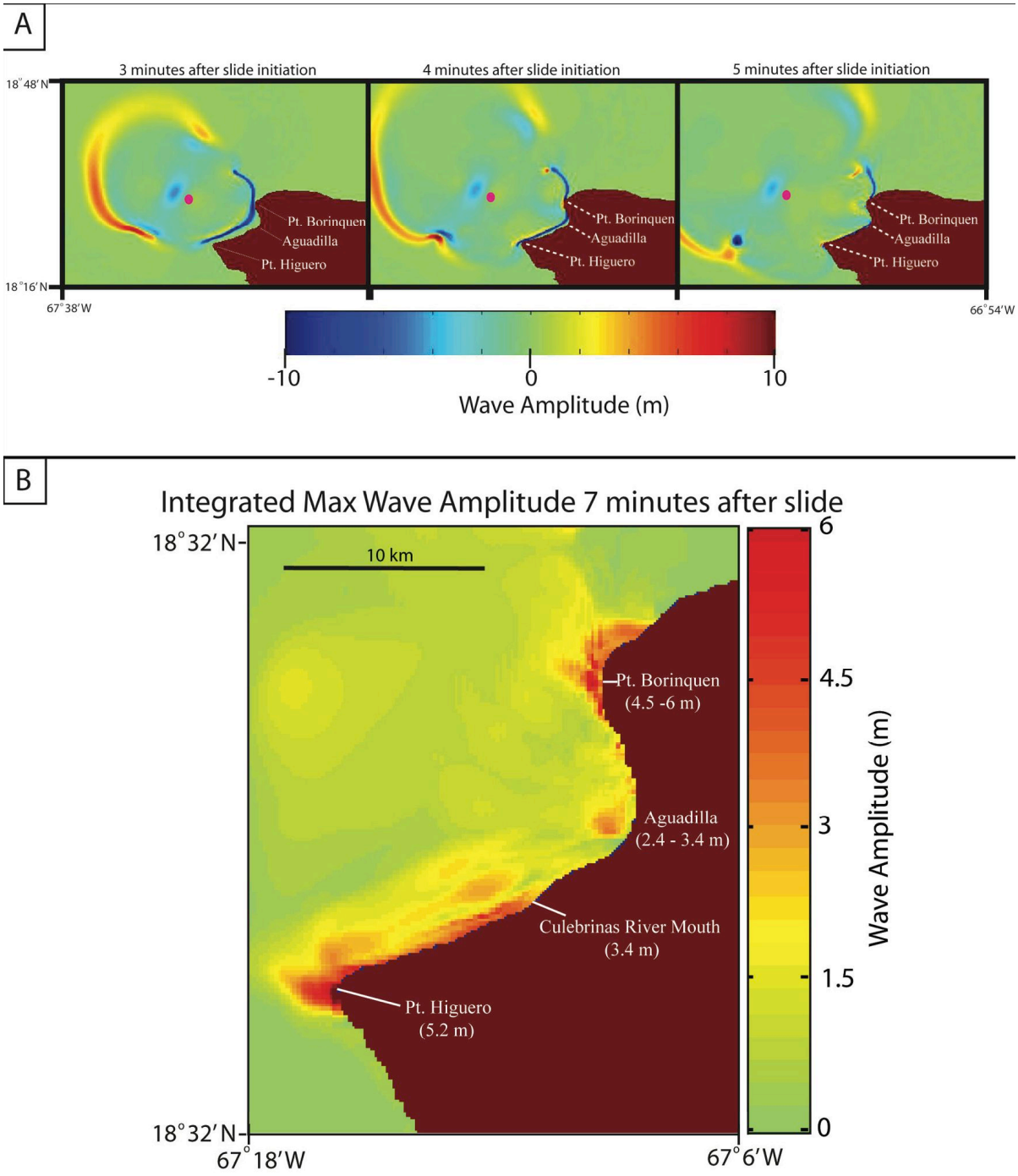

Figure 2. (A) Model results for a tsunami wave generated by a 6 km^3 slide showing the projected wave propagation pattern 3, 4, and 5 minutes after slide initiation. Wave amplitudes are in meters. The model shows a negative polarity wave initially arrives along the northwest coast of Puerto Rico, first at Pt. Borinquen, followed by Pt. Higuero and Aguadilla, consistent with first hand accounts (see Table 1). The pink dot represents the approximate location of the slide center at these time intervals. (B) Modeled wave amplitudes observed during the first 7 minutes of wave propagation for a 6 km^3 slide, with the highest wave amplitudes in red and the lowest in light green. Locations where known wave run-up values exist are also noted. In general, wave run-ups are consistent with observations (see Table 1).

resolution being limited to 150 m, and (2) limited constraints on the exact volume of the slide. By modeling what we believe is the largest slide that likely occurred (~6 km^3), we place an upper limit on run-up, since all else being equal, the larger the slide, the larger the wave [e.g. *Ward*, 2001]. To estimate possible error caused by bathymetry, we compare run-up values at multiple adjacent grid points, and use these difference to note potential run-up variability. To place constraints on the effect slide volume has on run-up, we also ran an additional model in which the height of the slide is reduced by half, resulting in a volume reduction of approximately 3 km^3.

Tsunami Model Results

We focus our results on calculated wave arrival times, phase, and run-up for the near-field tsunami wave at Pt. Borinquen, Pt. Higuero, Aguadilla, the three closest locations to the 6 km^3 slide, and the only locations impacted by the near-field tsunami where excellent observations of wave arrival times, wave phase, and run-up exist. Our analysis shows that the wave arrives first at Pt. Borinquen, 2.5-3.0 minutes after slide initiation, second at Pt. Higuero, ~3.5-4.0 minutes after slide initiation, and finally, at Aquadilla, 4.5-5.0 minutes after slide initiation (See Figure 2, and Table 1). At all locations, the initial arriving wave has a negative-to-positive phase. Wave run-up values indicate that the largest waves approaches Pt. Higuero (4.4 m +/- 1.7 m) and Pt. Borinquen (4.5 +/- 1 m), and finally Aguadilla (2.3 +/- 1.2 m) (Figure 2B, and Table 1). Similarly, model results for the 3 km^3 slide produced nearly identical wave arrival times, phase, and relative wave run-ups, however, absolute run-ups were reduced by ~60% compared to the 6 km^3 slide (Table 1).

Table 1. Comparison of observed vs. modeled amplitude, phase and arrival times

Location	Observed wave arrival time (min)	Modeled arrival time (min)	Observed phase	Modeled phase	Observed max wave run-up (m)	Modeled run-up for 6 km^3 slide and error (1 sigma) (m)	Modeled run-up for 3 km^3 slide and error (1 sigma) (m)
Pt. Borinquen	0 - 3	2.5 - 3	neg/pos	neg/pos	4.5 - 6	4.4 (+/-1.7)	2.0 (+/- 1.3)
Aguadilla	4 - 7	4.5 - 5	neg/pos	neg/pos	2.4 - 3.4	2.3 (+/-1.2)	0.9 (+/- 0.4)
Pt. Higuero	>3	3.5 - 4	neg/pos	neg/pos	5.2	4.5 (+/-1.0)	1.7 (+/- 0.4)

Did a slide trigger the 1918 Puerto Rico tsunami?

The modeled arrival times, wave phase, and run-ups generated by the slide are in good agreement with direct observations. The model indicates that a negative phase (ocean withdrawal) first arrives along the northwest coast of Puerto Rico (Figure 2A). Observers along the northwest corner of the island reported that the ocean drew-down several meters before inundating the coast a few minutes later, identical to model predictions.

Wave arrival times along the northwest coast of Puerto Rico also match observations, with the wave first arriving at Pt. Borinquen, followed by Pt. Higuero, Aguadilla. (Figure 2A, Table 1).

According to first-hand accounts, the shaking from the earthquake along the northwest coast lasted 2-3 minutes [*Reid and Taber*, 1919]. Assuming the slide occurred during the earthquake, wave arrival times are consistent with observations. For example, at Pt. Borinquen, ocean retreat was observed by the lighthouse keeper within three minutes and during the time of earthquake shaking [*Reid and Taber*, 1919], as predicted by our model. Likewise, the lighthouse keeper at Pt. Higuero observed the wave approach shore "shortly after" the earthquake, indicating that the wave likely arrived just after three minutes, also consistent with model results [*Reid and Taber*, 1919]. At Aguadilla, recorded wave arrival times range from four to seven minutes, and also match the 5 minute arrival time predicted by the model.

Model results for wave run-up assuming a 6 km^3 slide are also consistent with observations, with the largest run-ups observed at the Pts. Higuero and Borinquen followed by Aguadilla. High-water mark measurements along the northwest coast of Puerto Rico following the 1918 event suggest that the largest waves came ashore in the regions of Pt. Borinquen and Pt. Higuero, followed by the Aguadilla region, [*Reid and Taber*, 1919] (see Table 1 and Figure 2B). Furthermore, modeled wave run-up values for the 6 km^3 slide closely match observations and indicate that such a slide could generate the appropriate sized waves (Table 1).

To test the effect of slide size on wave run-up, we ran an additional model in which we reduced slide volume by 50%. This model resulted in nearly identical arrival times and phase with the original model, however, predicted wave run-up values were reduced on average by ~60% (Table 1), thereby indicating that a smaller slide may not be able to reproduce observed wave run-up values. Thus, we suggest that most if not all of the slide headwall must have failed to generate the observed near-field waves.

In spite of the relative simplicity of the slide model, which makes basic assumptions of slide shape, size and motion, the model replicates near-field observations of arrival time, phase, and run-up with considerable accuracy. The greatest errors in the model involve predicted run-up, as expected with a model where slide volume, local topography, and human factors (such as building locations and agricultural development zones) have a significant impact on run-up. Therefore, some discrepancy between predicted versus observed run-up is expected, provided first order estimates are generally consistent with observations.

Additional support for the slide triggering the tsunami is the strong evidence that a large slide occurred during the earthquake, i. e., the existence of multiple cable breaks and kilometer-length regions of buried cable in the vicinity of a well-imaged slide headwall. Whether this slide represents the primary source of the tsunami remains debatable. The fact that a submarine slide tsunami model generates a near-field wave with the appropriate arrival times, phase, and run-up along the northwest corner of Puerto Rico offers a compelling case that the slide may have played a key role in triggering the near-field portion of the 1918 tsunami, however, a more detailed study of the far-field wave is ultimately needed to determine if a slide can explain more distant tsunami observations. The occurrence of a concentrated wave run-up zone along the northwest coast of Puerto Rico, adjacent to the slide, is consistent with other near-field slide generated tsunami sources [e.g. *Heinrich et al.,* 2001*, Tappin et al.,* 1999]. Furthermore, the slide volume, which we estimate from bathymetry ranged between 2-6 km^3, is comparable in size with the 4 km^3 1998 Papua New Guinea slide that also generated a devastating yet regionally focused tsunami [*Heinrich et al.*, 2001; *Tappin et al.*, 1999].

The case for a submarine slide triggering the 1918 tsunami is compelling but equivocal. Not all slides generate tsunami, as noted by the fact that an aftershock 13 days after the 11 October 1918 earthquake triggered a second submarine slide that again broke cables in the same vicinity, yet no observed tsunami was reported [*Reid and Taber*, 1919]. Further analysis using higher resolution data over a greater modeling domain would be valuable. Some of the far-field tsunami run-up observations for the 1918 event, including those made in the Dominican Republic and Virgin Islands as well as the east coast of the US [*Reid and Taber*, 1919], may be difficult to reconcile with a slide-only scenario, since it seems counterintuitive that such a small slide could trigger a tsunami detected several thousands of kilometers away. Detailed analysis of these far-field observations requires further study that goes beyond the scope of this work.

Conclusions

Newly merged bathymetric and seismic data reveal a seafloor slide in the vicinity where multiple cable breaks occurred off the northwest coast of Puerto Rico during the 1918 earthquake. Comparison of near-field tsunami modeling results for this slide with historic observations of the tsunami produces a generally consistent match, and we suggest that a slide-generated tsunami in the cable-break region offers a viable alternative explanation for the observed near-field 1918 Puerto Rico tsunami. Submarine slide scarps are ubiquitous not only along Puerto Rico [*Grindlay et al.*, 2005; *ten Brink et al.*, 2006], but most continental margins including the Pacific Rim and Caribbean, where steep slopes exist and large tsunami occur frequently. Given that submarine slides are oftentimes triggered by earthquakes in these regions [*Meuneir et al.*, 2007], we postulate that they are perhaps more frequent tsunami generators than is commonly assumed. Our analysis highlights how high-resolution multibeam data coupled with side-scan sonar and seismic images can improve our understanding of earthquake-induced seafloor deformation, submarine sliding, and the tsunami generation. Future seismic analysis in the vicinity of the slide would place better constraints on slide volume and timing. Obtaining higher resolution bathymetric data over a broader region for far-field tsunami analysis, combined with coring and dating of slide debris would also help assess whether this slide ultimately triggered the 1918 tsunami.

Acknowledgements

We thank D. Doser for helpful conversations regarding character of the 1918 earthquake. This work was supported by NSF#OCE-9796189, UPR SeaGrant # R-122-1-04, UNCW's Center for Marine Science and Department of Geography and Geology, and the Geology Foundation at The University of Texas, Jackson School of Geosciences.

References:

Doser, D., et al. (2005), Historical earthquakes of the Puerto Rico--Virgin Islands region, in *Active tectonics and seismic hazards of Puerto Rico, the Virgin Islands, and offshore areas: Geological Society of America Special Paper 385*, edited by P. Mann, pp. 103-114, Geological Society of America.

Grilli, S. T., and P. Watts (1999), Modeling of waves generated by a moving submerged body. Applications to underwater landslides, *Engineering Analysis with Boundary Elements*, *23*, 645-656.

Grindlay, N. R., et al. (2005), A High Risk of Tsunami in the Northern Caribbean, *Eos*, *86*(12), 121,124.

Heinrich, P., et al. (2000), Near-field modeling of the July 17, 1998 tsunami in Papua New Guinea, *Geophys. Res. Let.*, *27*(19), 3037-3040.

Heinrich, P., et al. (2001), Numerical modelling of tsunami generation and propagation from submarine slumps: the 1998 Papua New Guinea event, *Geophys. J. Int.*, *145*, 97-111.

Ioualalen, M., et al. (2006), Numerical modeling of the 26 November 1999 Vanuatu tsunami, *J. Geophys. Res.*, *111*.

Jiang, L., and P. H. LeBlond (1992), The coupling of a submarine slide and the surface wave which it generates, *J. Geophys. Res.*, *97*(C8), 12731-12744.

Kanamori, H., and K. Masayuki (1993), The 1992 Nicaragua earthquake: a slow tsunami earthquake associated with subductioned sediments, *Nature*, *361*, 714-716.

Krause, D. C., et al. (1970), Turbidity currents and cable breaks in the western New Britain trench, *Geol. Soc. Amer. Bull.*, *81*, 2153-2160.

Mercado, A., and W. McCann (1998), Numerical Simulation of the 1918 Puerto Rico Tsunami, *Natural Hazards*, *18*, 57-76.

Meunier, P., N. Hovius, and A. J. Haines (2007), Regional patterns of earthquake-triggered landslides and their relation to ground motion, *Geophy. Res. Let.,34*(L20408)

Pacheco, J. F., and L. R. Sykes (1992), Seismic Moment Catalog of Large Shallow Earthquakes, 1900 to 1989, *Bull. Seismol. Soc. Amer.*, 82(3), 1306-1349

Reid, H. F., and S. Taber (1919), The Porto Rico earthquakes of October-November 1918, *Bull. Seismol. Soc. Amer.*, *9*(4), 94-127.

Tappin, D. R., et al. (1999), Sediment slump likely caused 1998 Papua New Guinea tsunami, *EOS*, *80*(30), 329,334,340.

ten Brink, U. S., et al. (2006), Size distribution of submarine landslides and its implication to tsunami hazard in Puerto Rico, *Geophys. Res. Let.*, *33*(L11307).

Tinti, S., et al. (1999), Numerical simulation of the landslide-induced tsunami of 1988 on Vulcano Island, Italy, *Bull. Volcanology*, *61*, 121-137.

Ward, S. N. (2001), Landslide tsunami, *J. Geophys. Res.*, *106*(6), 11201-11215.

Watts, P. (1997), Water waves generated by underwater landslides, California Institute of Technology, Pasadena. Ph.D Thesis

Watts, P., et al. (2005), Tsunami generation by submarine mass failure. II: Predictive equations and case studies, *J. of Waterway, Port, Coastal, and Ocean Engineering*, *131*(6), 298-310.

TSUNAMIGENIC SOURCES IN THE INDIAN OCEAN

R. K. Jaiswal[1], B. K. Rastogi[1] & Tad S. Murty[2]
[1]Institute of Seismological Research, Gandhinagar-382 018, Gujarat (India)
[2]University of Ottawa, Ottawa, Canada
Email: rajeev_ngri@rediffmail.com

ABSTRACT

Based on an assessment of the repeat periods of great earthquakes from past seismicity, convergence rates and paleoseismological results, possible future source zones of tsunami generating earthquakes in the Indian Ocean (possible seismic gap areas) are identified along subduction zones and zones of compression. Central Sumatra, Java, Makran coast, Indus Delta, Kutch-Saurashtra, Bangladesh and southern Myanmar are identified as possible source zones of earthquakes in near future which might cause tsunamis in the Indian Ocean, and in particular, that could affect India. The Sunda Arc (covering Sumatra and Java) subduction zone, situated on the eastern side of the Indian Ocean, is one of the most active plate margins in the world that generates frequent great earthquakes, volcanic eruptions and tsunamis. The Andaman-Nicobar group of islands is also a seismically active zone that generates frequent earthquakes. However, northern Sumatra and Andaman-Nicobar regions are assessed to be probably free from great earthquakes ($M \geq 8.0$) for a few decades due to occurrence of 2004 Mw 9.3 and 2005 Mw 8.7 earthquakes. The Krakatau volcanic eruptions have caused large tsunamis in the past. This volcano and a few others situated on the ocean bed can cause large tsunamis in the future. List of past tsunamis generated due to earthquakes/volcanic eruptions that affected the Indian region and vicinity in the Indian Ocean are also presented.

1. INTRODUCTION

From GPS data, Subarya et al. (2006) inferred that the Sumatra-Andaman earthquake of 26 December 2004 was generated by rupture of the Sunda subduction megathrust over a length of 1500 km, width of <150 km and a slip exceeding 20m offshore of northern Sumatra, mostly at depths shallower than 30 km. Stein and Okal (2005), Lay et al. (2005) and Ammon et al. (2005) inferred a rupture length of 1300km, width of 160-240km and slip of 5-20m from seismological data. The rupture was wide in Sumatra and Nicobar segments (up to 260km width between the subduction front and Sumatra Fault) but narrows down to 160km in the Andaman segment (between the subduction front and West Andaman Fault) that is mapped east of Andaman Islands by Curray (2005). The tsunami due to this giant earthquake of magnitude Mw9.3 traveled throughout the Indian Ocean with large run up and was the most destructive in history causing some 300, 000 deaths. This tsunami has created great interest in predicting future occurrences of such tsunamis. Tectonics, seismicity and seismic gap areas of different earthquake belts in the Indian Ocean are assessed to infer future possibilities of tsunami generation.

List of past tsunamis generated due to earthquakes/volcanic eruptions that affected the Indian region and vicinity in the Indian Ocean are listed in Table 1 and also shown in Fig.1. Thrust type earthquakes along subduction zones that cause vertical movement of the ocean floor are usually tsunamigenic (Rastogi, 2005a, b). Such zones in the Indian Ocean are in Andaman-Nicobar region, Sumatra-Java region and Makran coast (Fig.2). Volcanic eruptions along the Sunda Arc can give rise to large tsunamis. Thrust-type earthquakes occurring along coastal zones of compressive stress along the Indus delta and Kutch-Saurashtra region in the west and Myanmar-Bangladesh border region in the east have given rise to occasional tsunamis and can again generate tsunamis in future. Minor tsunamis can be generated due to dip-slip faulting along oceanic ridges. The tectonics and seismicity in these zones are briefly discussed and long-term assessment of future great tsunamigenic earthquakes in these zones is presented.

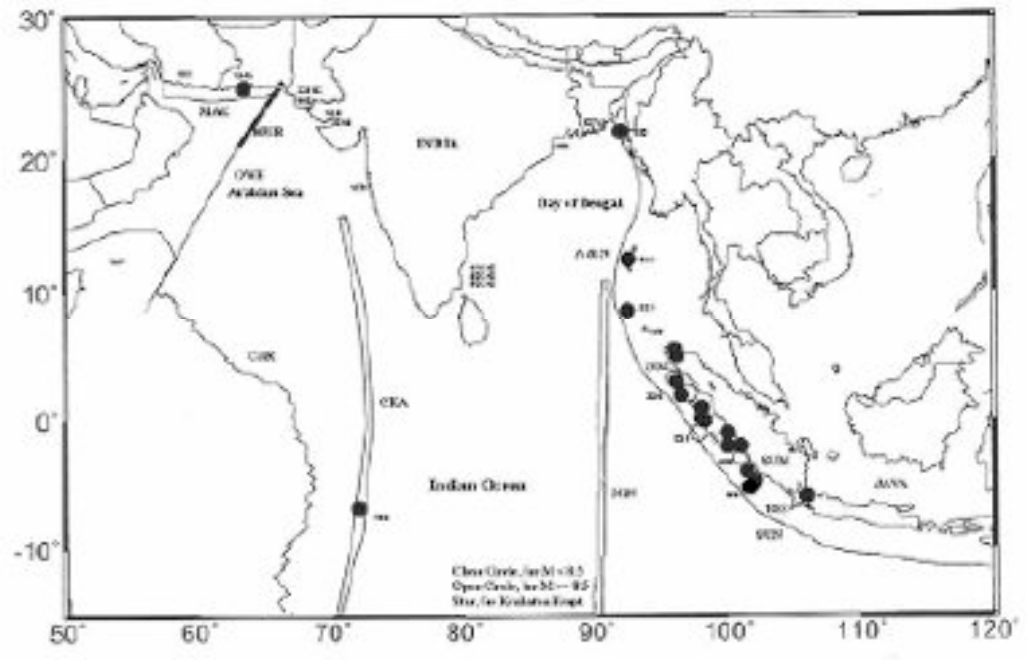

Fig.1. Locations of tsunamis generated due to earthquakes/volcanic eruptions that affected Indian region and vicinity in the Indian Ocean.

Fig.2. Rupture areas of great earthquakes of Mw□ 7.7 and inferred seismic gap areas that could be sites of future tsunamigenic great earthquakes in the Indian Ocean

2. TSUNAMIGENIC EARTHQUAKE SOURCE ZONES IN THE INDIAN OCEAN

The Sunda Arc

The Sunda Arc (Java, Sumatra and Lesser Sunda subduction zone) is one of the most active plate tectonic margins in the world, accommodating 67±7mm/yr, N11°E convergence (derived from GPS surveys) between the South Asian and India/Australian plates, which arcs 5,500 kilometers from Myanmar past Sumatra and Java toward Australia (Tregoning et al., 1994). Many characteristics of Sunda Arc change significantly along strike. Interplate motion normal to the arc near Java, becoming oblique at Sumatra, where motion parallel to the arc is accommodated by dextral strike-slip displacement along the Sumatra fault system lying parallel and north of the convergent margin (Newcomb and McCann, 1987). The plates meet 5 kilometers beneath the sea at the Sumatran Trench, on the floor of the Indian Ocean. The trench runs roughly parallel to the western coast of Sumatra and southern coast of Java, about 200 kilometers offshore. At the trench, the Indian/Australian plate is being subducted; that is, it is diving into the earth's interior and being overridden by Southeast Asia. The contact between the two plates is a “megathrust”. The two plates do not glide smoothly past each other along the megathrust but move in "stick-slip" fashion. This means that the megathrust remains locked for decades or centuries, and then slips suddenly a few (or a few tens of) meters, generating a large earthquake. Some coastal areas east of the megathrust sink by a meter or so, leading to permanent swamping of previously dry, habitable ground. Islands above the megathrust rise a few meters, so that shallow coral reefs emerge from the sea.

Newcomb and McCann (1987) identified from historic records two great interplate earthquakes (1833, Mw 8.7 and 1861, Mw 8.5) which ruptured 400-600km segments of the Sumatra fore arc. Great past Sumatran earthquakes in 1797 (Mw 8.2) and 1833 (Mw 8.7) produced large tsunamis on the islands and mainland coast (Newcomb and McCann, 1987). They also identified many other major and moderate earthquakes in Sunda Arc. Prior to their study, Sumatra was characterized as relatively aseismic due to lack of great earthquakes in the instrumental era. Java and Lesser Sunda islands had major earthquakes (Ms 6) in the historic record, but none as big as the great events near Sumatra.

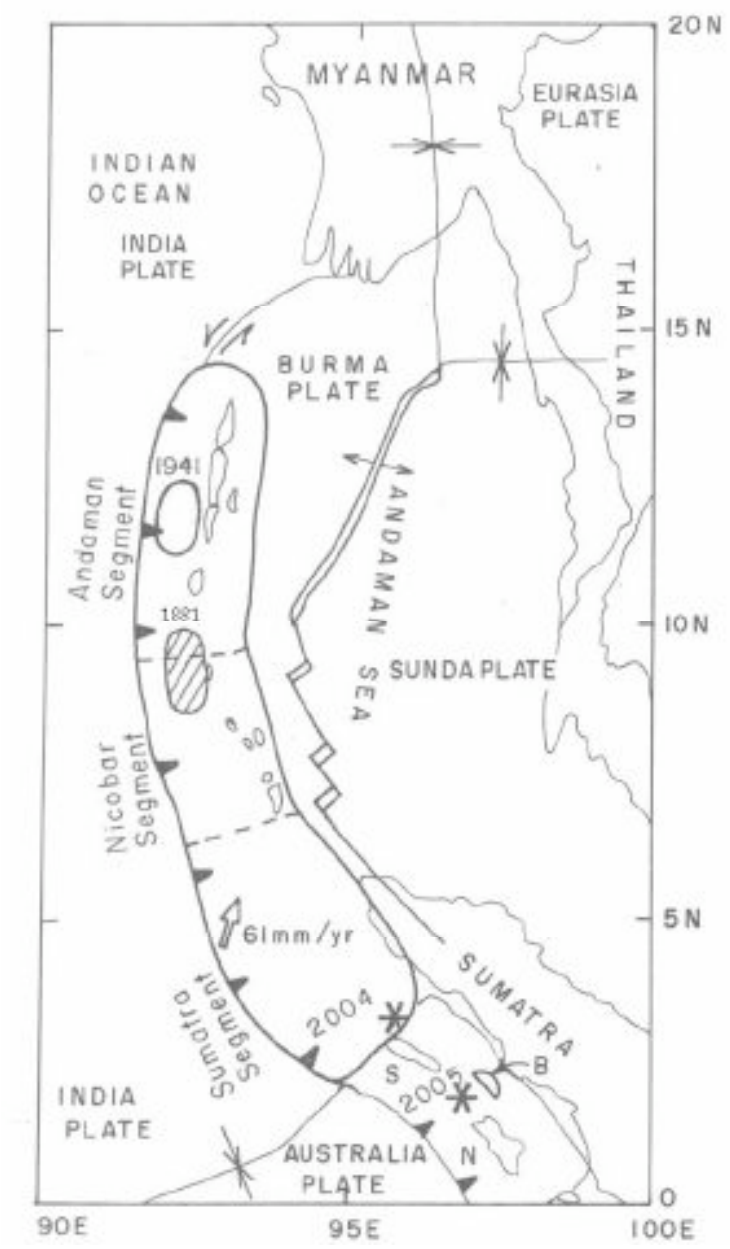

Fig. 3. Source zones of 2004 and 2005 earthquakes in Sumatra – Andaman Arc. Three of the Mentawai islands are Simeuleue (S), Banyak (B) and Nias (N). Rupture zone for 2004 earthquake is taken from Lay et al. (2005) and Stein and Okal (2005) and rupture zone for 2005 earthquake is taken from Ammon et al. (2005).

From coral uplift data Zachariasen et al. (1999) estimated the magnitude of the 1833 earthquake to be between 8.8 and 9.2. They also estimated a return period of such a giant earthquake to be 265 yr. They derived this interval by dividing the estimated slip of 13m by the rate of subduction. To estimate the rate of subduction, they subtracted the slip vector of the Great Sumatra Fault (11mm/yr, S35°E, Sieh et al. 1991) from relative plate velocity (67mm/yr, N11°E). The resultant vector for the subduction zone was 60mm/yr, N18°E. The component of this vector perpendicular to the subduction zone is 49mm/yr, N54°E. At a rate of 49mm/yr, 13m of slip would occur about every 265yr. However, it is noticed that ~M8 earthquakes and tsunamis have recurred more frequently. Great earthquakes occurred in 1797 (M8.2), 1833 (M8.7), 1861 (M8.5), 2000 (Mw 7.8), 2004 (Mw 9.3), 2005 (Mw 8.7) (Figs. 3 and 4).

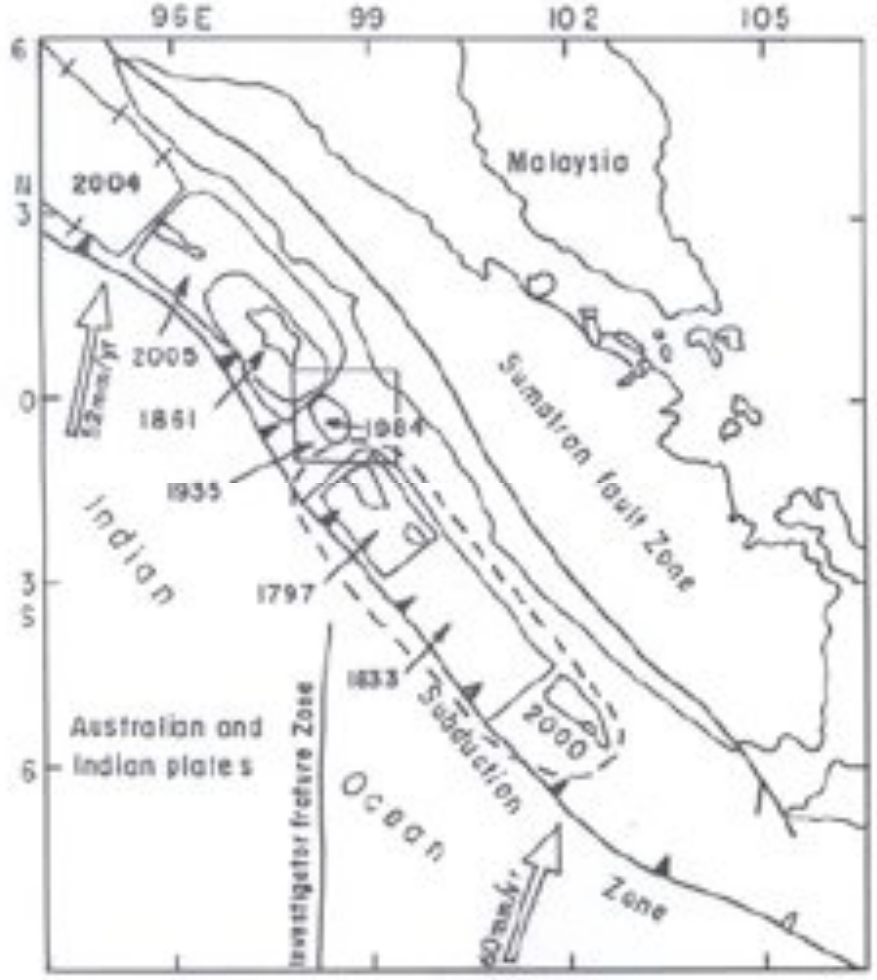

Fig. 4. Rupture areas of past great earthquakes along Sumatra. The Southern Sumatra zone marked by broken line was a possible site for future tsunamigenic great earthquake as earthquake of Mw 8.4 September 12, 2007 occurred 130 km off the SW of Bengkulu, Sumatra, Indonesia (4.52 °S, 101.374 ° E, NEIC) followed by two major earthquakes of Mw 7.9 (2.506°S, 100.906°E, NEIC) and Mw 7.1 (2.160°S, 99.588°E, NEIC) within 12 hrs and 15 hrs after the occurrence of Mw8.4 event within the rupture zone of past great earthquakes of 1833 and 1797 occurred in this broken line. This is presented by Rastogi & Jaiswal (2005) in IGU Jaiswal & Rastogi (2006) in ASC. Rupture zones of different earthquakes are taken from Natawidjaja et al. (2004) and Zachariasen et al. (1999).

The locations of some of these earthquakes are the same or overlapping. The giant earthquakes of M≥8.5 encompass the rupture zones of M~8 earthquakes of past decades as if these did not occur at all. For example the 1833 earthquake rupture encompassed rupture zone of the Mw 8.2 earthquake that occurred only 36 years earlier. Similarly the 2004 rupture encompassed rupture zones of 1881 Nicobar earthquake and 1941 Andaman earthquake. The 2005 M8.7 rupture has recurred in the same area as that of 1861 rupture for M8.5 earthquake after only 144 years. It indicates that great earthquakes can recur every few decades. Rastogi and Jaiswal (2005) & Jaiswal and Rastogi (2006) recognized that southern Sumatra (rupture zone of 1833 and 1797) has the potential for a great earthquake based on assessment of repeat periods of great earthquakes from past seismicity, convergence rates of subduction zone and paleoseismological results which are shown in Fig. 2 and Fig. 4 and marked by the broken line. However, the effect of tsunamis due to these earthquakes in India and Sri Lanka may be a limited one as the path of the tsunami will be oblique to the rupture zone. This became true as a great earthquake of Mw 8.4 struck 130 km off the SW of Bengkulu, Sumatra, Indonesia on September 12, 2007 (4.52° S, 101.374° E, focal depth 34km, NEIC) at 11:10:26 UTC (16:40:26 IST), killing 9 people and injured few tens, generated a relatively small tsunami near the epicentral zone followed by two major earthquakes of Mw 7.9 (2.506° S, 100.906° E, 30km, NEIC) and Mw 7.1 (2.160° S, 99.588° E, 22km, NEIC) within 12 hrs and 15 hrs after the occurrence of Mw 8.4 event within the rupture zone of past great earthquakes of 1833 and 1797. Since the Indian & Sri Lankan mainlands were not perpendicular to the rupture zone of the minor tsunami due to the earthquake of September 12, 2007 generating NW-SE oriented fault plane hence directivity of this tsunami is towards the SW and the tsunami with the maximum amplitude propagated in the SW direction.

The possible locales for near future earthquakes are seismic gap areas that have remained un-ruptured in the past few decades. The 2004 Sumatra earthquake occurred in one such gap (Fig.2). Kerry Sieh (CALTECH website) and Satyanarayana and Rastogi (2005) recognized that a segment of the subduction zone south of it as a possible site for a future great earthquake. The 28 March 2005 earthquake of M8.7 occurred in this gap (Fig.4). The boundary between rupture zones of 2004 and 2005 earthquakes is marked by a deep fracture named as Investigator fracture zone. The rupture zones of these two earthquakes have covered Northern Sumatra and Andaman-Nicobar regions, which are now assessed to be probably free from great earthquakes (M≥8.0) for a few decades (Rastogi, 2005b). Natawidjaja et al. (2006) recognized that the threat of another giant earthquake is high off central Sumatra. Pollitz et al. (2006) computed stress changes during co-seismic and post-seismic deformation after the occurrence of the 2004 and 2005 great Sumatran earthquake in order to focus on post-seismic deformation that is driven by viscoelastic relaxation of low viscosity asthenosphere. The December 26, 2004 Sumatra earthquake increased CFS (Coulomb Failure Stress) by 0.25 bar near the nucleation zone of the March 2005 earthquake at ~40km depth could be the region of occurrence of March 2005 earthquake. Co-seismic stress around 1797 and 1833 events of Sunda trench was negligible but post-seismic stress perturbation in CFS increased by 0.1 to 0.2 bars around these rupture zones between 2 to 8 year after the December 2004 event (Pollitz et al., 2006). They found that predicted the CFS increased by >0.1 bar over Sunda trench in coming years, raising seismic hazards along certain patches which already have a substantial amount of accumulated stress.

Co-seismic stress changes due to the 2004 event increased the stress may migrate farther south as a result of viscoelastic relaxation in the lower crust (McCloskey et al., 2005; Nalbant et al., 2005). Nalbant et al. (2005) also evaluated the stress at the hypocenter of 2005 earthquake induced by Sumatra-

Andaman rupture and found it to be between 0.07 and 0.17 bars. The size of this triggering stress reveals the extreme complexity and non-linearity of the earthquake nucleation process.

Two Sumatran events of 2004 and 2005 altered the state of stress near the surrounding region of earthquakes could be the probable cause of generating Simeulue, Indonesia earthquake of M7.4 on February 20, 2008 (2.778° N, 95.978° E, depth 35km, NEIC), epicenter located at 59km south of 2004 event and 139km NW of 2005 event. Stress changes indicate that greatest current seismic threat comes from the Mentawai segment between about 0.7 and 5.5° S (Nalbant et al., 2005).

Farther south in southern Sumatra and Java large earthquakes are possible in future (Ammon, 2006). Between latitudes of 1-6° S large/great earthquakes occurred during 1797 and 1833 and hence a great earthquake can be expected within a few decades now. Zachariasen et al. (2000) inferred from the study of coral microatolls that the Mentawai Islands in this region are submerging at rate of 4 – 10 mm/yr over five decades and the elastic strain is accumulating in the interseismic period. The northern Sumatra and Andaman-Nicobar regions may not experience great earthquakes for a few decades as 2004 Mw 9.3 and Mw 8.7 earthquakes have ruptured the entire 1600km length of the subduction zone from Andaman to northern Sumatra. However the possibility of an earthquake of magnitude 7.0-7.5 on the Sumatra fault north of 4° N has not receded (Nalbant et al., 2005).

Andaman-Nicobar Arc

The Sunda Arc extends further north to the region of Andaman-Nicobar group of islands, which is also seismically active zone and generates frequent large earthquakes. Large earthquakes in 1847 (Mw>7.5), 1868, 1881 (Mw7.9) and 1941 (M7.7) generated tsunamis. The convergence rates estimated
by GPS measurements indicate repeat periods of 114-200 yr for great earthquakes (Ortiz and Bilham, 2003).

The Andaman and Nicobar islands form an island arc or ridge and are made up of ophiolites and sediments scraped off the down going Indian plate. The ridge lies on the Andaman plate as referred to by Dasgupta (1993) or Burma plate (as referred by Curray et al. 1982). The ridge is bound to the east by the Sunda plate boundary, that has strike-slip faults and spreading centers, and to the west by the subduction zone of the Indian plate (Fig. 5). At latitude 9° N the Indian plate converges at N 23° E obliquely toward the Asian plate at 54 mm/yr (DeMets et al., 1990, 1994). Further north the convergence is nearly perpendicular to the subduction zone. Between little Andaman and Car Nicobar at around 10° N, there are imbricate N-S trending thrust sheets dipping east. These thrusts are extending north and south for long distances and may be causing uplift of beaches in Car Nicobar. The Sumatra fault continues up to Nicobar. North of 10.2° N the fault is offset 100km eastward by the Andaman spreading center and becomes inactive. North of 10° N, the Benioff zone, west of the Andamans, is clearly expressed by microseismicity to 100km depth. Between 10° to 12° N, back arc spreading zone is also depicted by microseismicity (Ortiz and Bilham, 2003).

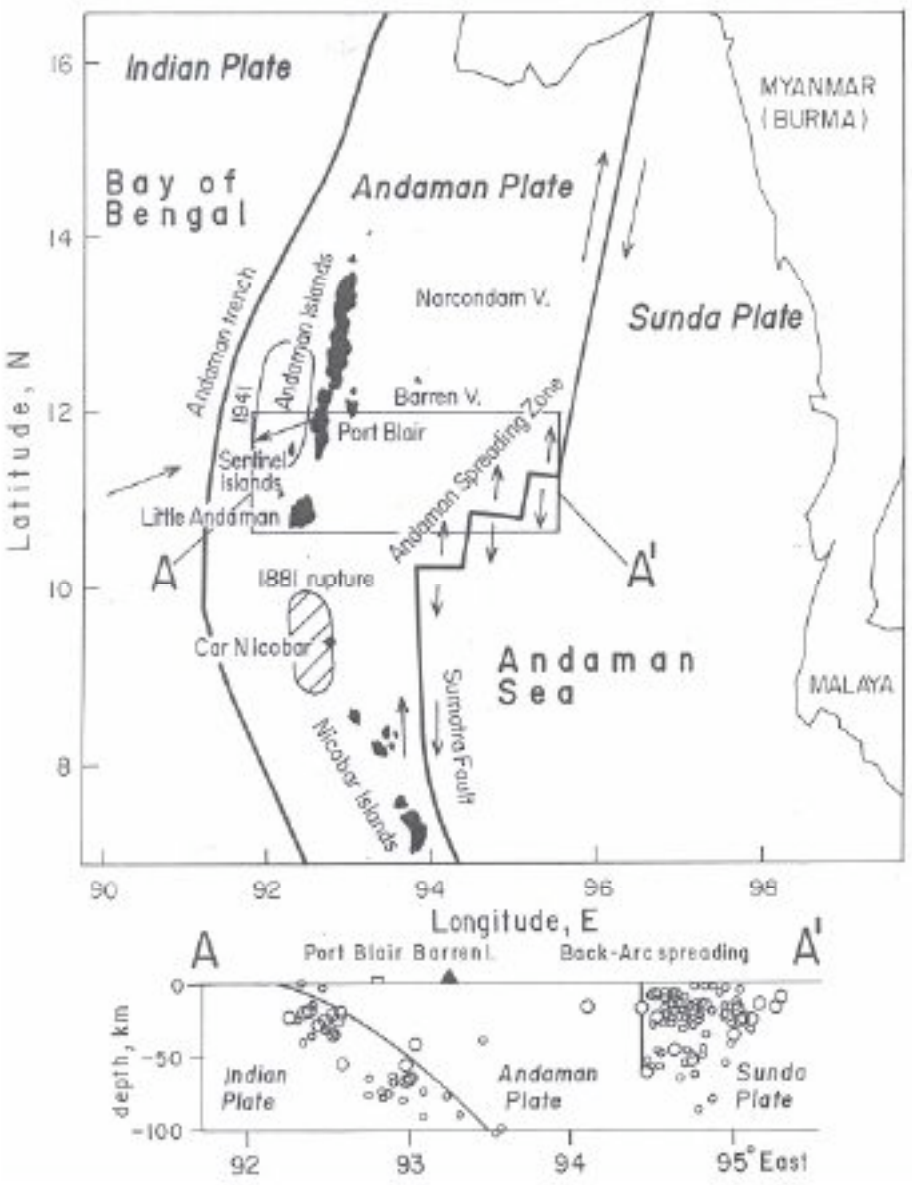

Fig. 5. The location of 1941 earthquake near Andaman Islands and 1881 earthquake near Car Nicobar are indicated. Seismicity between 10.8□N and 12□N are shown from Engdahl et al. (1998). The figure is from Ortiz and Bilham (2003).

The Makran Subduction Zone

The Makran subduction zone of Iran and Pakistan (boundary between Iran and Pakistan runs roughly N-S at about 62° E) is seismically less active but has produced great earthquakes and tsunamis. Great earthquakes of rupture lengths of about 200km each have occurred in 1483 (Long. 58 – 60□E), 1851 (Long. 61 - 63° E), 1945 (Long. 63 - 65° E) and 1765 (Long. 65 - 67° E) (Byrne et al. 1992). A tsunami is known to have occurred in Iran coast in 1008 (Murty et al. 1999). The 28 Nov. 1945 (Mw 8.0) earthquake generated the last major tsunami in the Arabian Sea. More than 4000 people were killed

on the Makran coast by both the earthquake and the tsunami. The run up in Makran was 17m and at Kutch 11m. The tsunami caused damage in Bombay (now called Mumbai) with 2 m run up and affected Karwar (Karnataka) (Pendse, 1945; Mathur, 1998). This earthquake occurred in the eastern part of the Makran zone, two sides of which remain potential zones for great earthquakes. The Makran subduction zone is one of the largest sedimentary accretionary wedges on earth, covered with up to 7 km of thick sediments. Due to sudden slumping along Makran accretionary wedges with large amount of sediments may generate a large tsunami, somewhat similar to the 1992 Nicaragua earthquake of M_s 70-7.3 (Piatanesi et al. 1996) which generated a large tsunami due to fall of accretionary wedges.

The earthquake of 1945 in Eastern Makran is an interplate thrust event that ruptured approximately 1/5th of the length of the Makran subduction zone. Several earthquakes in this region show thrust mechanism The western Makran zone has no clear record of historic great earthquakes and modern instruments have also not detected shallow thrust events. Most earthquakes in western Makran occur within the down-going plate at intermediate depth.

Absence of plate boundary earthquakes in western Makran indicates either that entirely aseismic subduction occurs or that the plate boundary is currently locked and experiences great earthquakes with long repeat times. Evidence is presently inconclusive without GPS measurements and knowledge of velocity structure. However, presence of well-defined late Holocene terraces along portions of the coasts of eastern and western Makran could be interpreted as evidence that both sections of the arc are capable of generating large plate boundary earthquakes (Byrne et al. 1992).

Source Zones of Indus Delta, Kutch-Saurashtra and Bangladesh-Myanmar Regions

Our study indicates that the Indus delta and probably also the coasts of Kutch and Saurashtra are also potential zones for great thrust-type earthquakes and tsunamis. In May 1668 the Indus delta town of Samawani (or Samaji) with 30,000 houses was sunk due to an earthquake (Oldham, 1883) of magnitude 8. There might have been a tsunami to drown the coastal town. The 16 June 1819, Mw 7.8 and 19 June 1845 M7 earthquakes in Kutch probably caused tsunamis (Macmurdo, 1821; Nelson, 1846; Rastogi and Jaiswal, 2006). An earthquake in 1762 in Myanmar generated a tsunami and an earthquake in 1874 near Bangladesh had likely generated a tsunami. Some earthquakes in future also in these regions can possibly generate tsunamis.

Cummins (2007) observed similar pattern of generation of megathrust tsunamigenic earthquake along the coast of Myanmar as in the other parts of the subduction zones of the world. According to him the seismogenic zone of the Andaman-Nicobar subduction zone extends beneath the Bengal fan. Guzmn-Speziale and Ni (2000) interpreted that there is no active subduction between the Indian plate and Southeast Asia and suggested that all of the relative motion between the Indian and Eurasian plates is accommodated along the Sagaing fault in central Myanmar. But Global Positioning System (GPS) surveys suggested that only 60% of the relative plate motion is accommodated along the Sagaing fault and the remaining either by distributed deformation west of the Sagaing fault, or by locking of the Arakan subduction zone (Socquet et al. 2006; Vigny et al., 2003). According to GPS survey the Arakan subduction zone would be expected to produce a magnitude 8.5 earthquake every century or a magnitude 9 every 500 years (Socquet et al. 2006).

The northern Bay of Bengal is having a unique structure because it contains the world's largest submarine fan system i.e. called Bengal Fan, consisting of sediments that have been shed off Tibet and the Himalayas since the Early Miocene. The thickness of the Bengal Fan sediments reaches up to 20 km (Alam et al., 2003). Because even a 1-km-thick sediment cover can insulate the underlying plate enough to cause significant up-dip extension of the thermal regime required for seismogenesis (Wang et al., 1995).

One cannot be certain that the 1762 earthquake produced destructive tsunami; however the rapid rate of sedimentation in the Bay of Bengal could generate tsunamis caused by submarine landslides similar to other part of the world (Cummins, 2007). With the evidence of active convergence along a coastal region with an extremely high population density suggests that the risk of a major tsunami in the northern Bay of Bengal should be taken into consideration seriously.

Carlsberg Spreading ridge and Older Oceanic Ridges

Normal fault type earthquakes can also generate moderate tsunamis. Strike-slip earthquakes that cause horizontal movement of the ocean floor are not tsunamigenic but oblique-slip/dip-slip component in them can generate weak tsunamis. The Carlsberg spreading ridge and relics of past plate movements like Ninety-East ridge and Chagos ridge are sites of such earthquakes. The Chagos ridge east of Carlsberg ridge had given rise to a local tsunami due to a normal faulting earthquake of Mw 7.7 of 30 Nov. 1983 near Diego Garcia (Fig. 6). Hence, local tsunamis are possible in these regions.

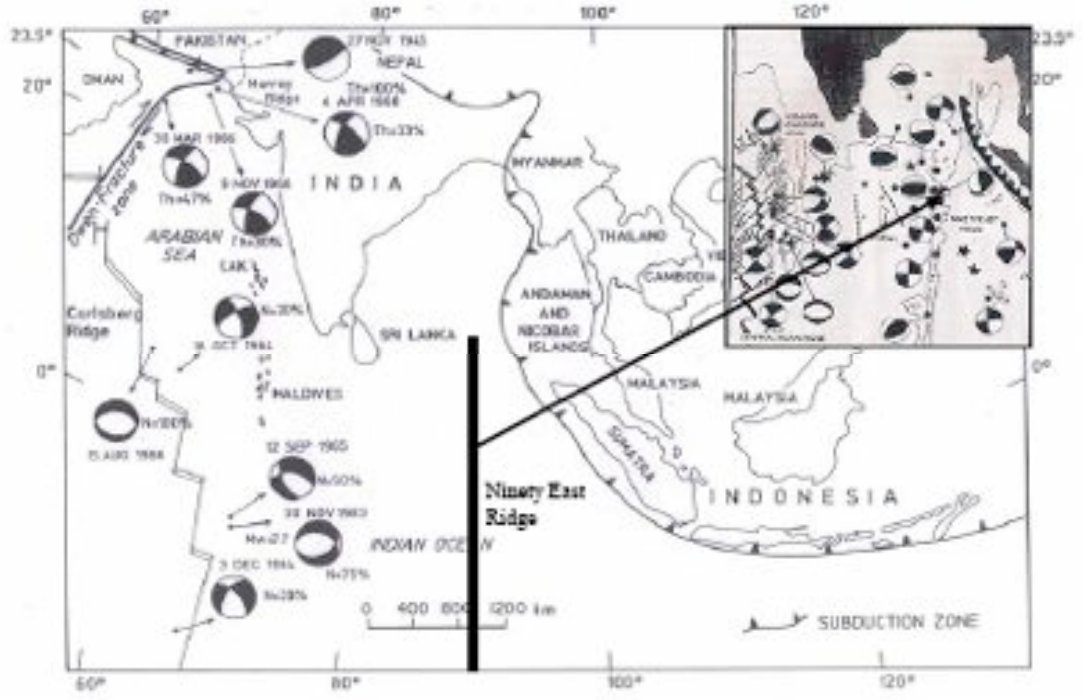

Fig. 6. Tectonic framework of the entire Indian Ocean and the focal mechanisms along the ridges in the Indian Ocean which indicate dip-slip component.

3. TSUNAMIS DUE TO VOLCANIC ERUPTIONS

The Sunda Arc (Indonesia) has the largest number of historically active volcanoes (76), has a total of 1,171 dated eruptions (Four fifths in the twentieth Century) and has suffered the highest number of damaging eruptions. However, most of the volcanoes are not on ocean bed and hence are not known to have caused tsunamis, except the Krakatau volcano. The renowned Krakatau volcano lies in the Sunda Strait between Java and Sumatra. The Krakatau eruptions in the third century AD (Chinese records), 416 AD (forming a 7km wide caldera), one between 416 AD and 1883, 1883 (7kmx5km caldera), 1927 and 1928 has caused tsunamis *(Smithsonian Institution Global Volcanism Program Website, 2000)*.

According to ancient Japanese scriptures, the first known super colossal eruption of Krakatau occurred in the year 416 A. D. – Some have reported it to occur in 535 A.D. The energy of this eruption is estimated to have been about 400 megatons of TNT, or the equivalent of 20,000 Hiroshima bombs. This violent early eruption destroyed the volcano, which collapsed and created a 7 km wide submarine caldera. The remnants of this earlier violent volcanic explosion were the three islands of Krakatau, Verlaten and Lang. Undoubtedly the 416 A.D. eruption generated a series of catastrophic tsunamis, which must have been much greater than those generated in 1883. However, there are no records to document the size of these early tsunamis or the destruction they caused, except possibly a description from India.

Subsequent to the 416 A.D. eruption and prior to 1883, three volcanic cones of Krakatau and at least one older caldera had combined again to form the island of Rakata probably due to a large eruption. The volcanic cones on the island were aligned in a north-south direction. Overall approximate dimensions of the island were 5km x 7km (Pararas-Carayannis, 2003).

The historic record shows that the strongest tsunami was associated with the volcanic eruption of Krakatau in Indonesia on 27 Aug. 1883. The 35m-high tsunami took a toll of 36,000 lives in western Java and southern Sumatra. The island volcano of Krakatau exploded with devastating fury, blowing its underground magma chamber partly empty so that much overlying land and seabed collapsed into it forming a 7-km wide caldera. Tsunami waves were observed throughout the Indian Ocean, the Pacific Ocean, the American West Coast, South America, and even as far away as the English Channel. On the nearby coasts of Java and Sumatra the sea flood went many kilometers inland.

Subsequent local tsunamis in the Sunda Strait were generated by the 1927 and 1928 eruptions of the new volcano of Anak Krakatau (Child of Krakatau) that formed in the area.

4. CONCLUSION

Northern Sumatra and Andaman-Nicobar regions are assessed to be probably ($M \geq 8.0$) free from great earthquakes for a few decades due to occurrence of 2004 Mw 9.3 and 2005 Mw 8.7 earthquakes. However, stress altered due to 2004 and 2005 event in the surrounding region can generate earthquakes of magnitude $M \leq 7.5$. Central Sumatra & Java has potential for a tsunamigenic earthquake in future. However, the effect of tsunami due to this in India and Sri Lanka may be a limited one as the path of tsunami will be oblique to the rupture zone. Eastern and western parts of the Makran subduction zone of southern Pakistan are potential zones for great earthquakes that can generate tsunamis affecting west coast of India. The eastern part of the Makran zone has produced the 1945 Mw 8.0 earthquake that generated the last major tsunami in the Arabian Sea. Some sectors of the Makran zone are un-ruptured for a long time and can produce large earthquakes in near future. Indus Delta and may be the coasts of

Kutch and Saurashtra are also potential zones for great earthquakes and tsunami. Earthquakes in the southernmost Myanmar and Bangladesh have generated tsunamis in the past. Earthquakes in future also in these regions can possibly generate tsunamis.

5. ACKNOWLEDGEMENT

The work was carried out under a project sponsored by Dept. Sc. Tech., New Delhi.

6. REFERENCES

Alam, M., M. M. Alam, J. R. Curray, Rahman Chowdhury, M. L. and M. Royhan Gani, (2003). An overview of the sedimentary geology of the Bengal Basin in relation to the regional tectonic framework and basin-fill history, Sedim. Geol., 155, 179–208.

Ammon, C. J., (2006). Megathrust investigations, Nature, 440, 31-32.

Ammon, C. J., Chen Ji, H. K. Thio, D. Robinson, S. Ni, V. Hjorleifsdottir, H. Kanamori, T. Lay, S. Das, D. Helmberger, G. Ichinose, J. Polet and D. Wald, (2005). Rupture process of the 2004 Sumatra-Andaman earthquake, Science, 308, 1133-1139.

Banghar, A.R. and L.R. Sykes, (1969). Focal mechanisms of earthquakes in the Indian Ocean and adjacent regions, J. Geophys. Res., 74, 632-649.

Bendick, R. and R. Bilham, (1999). A Search for Buckling of the SW Indian Coast related to Himalayan Collision, in Macfarlane, A., Sorkhabi, R. B., and Quade, J., eds., Himalaya and Tibet: Mountain Roots to Mountain Tops: Geol Soc Amer. Special paper 328. 313-322.

Berninghausen, W. H., (1966). Tsunamis and Seismic Seiches reported from regions adjacent to the Indian Ocean, Bull. Seism. Soc. Am., 56 (1), 69-74.

Bilham, R, R. Engdahl, N. Feld and S. P. Satyabala (2005). Partial and complete rupture of the Indo-Andaman plate boundary 1847-2004, Seism. Res. Lett., 76 (3), 299-311.

Byrne, D. E., L. R. Sykes and D.M. Davis, (1992). Great thrust earthquakes and aseismic slip along the plate boundary of the Makran subduction zone, J. Geophys. Res., 97, 449-478.

Commins, P.R., (2007). The potential for giant tsunamigenic earthquakes in the northern Bay of Bengal, Nature, 449, doi:10.1038/nature06088.

Curray, J. R., F. J. Emmel, D. G. Moore and R. W. Raitt, (1982). Structure, tectonics and geological history of the NE Indian Ocean, in The Ocean Basins and Margins, vol. 6, The Indian Ocean, edited by A. E. M. Nairn and F. G. Sehli, pp. 399–450, Plenum, New York.

Curray, J. R., (2005). Tectonics and history of the Andaman sea region, J. Asian Earth Sc., 25, 187-232.

Dasgupta, S., (1993). Seismotectonics and stress distribution in the Andaman Plate, Mem. Geol. Soc. India, 23, 319–334.

DeMets, C., R. G. Gordon, D. F. Argus and S. Stein, (1990). Current plate motions, Geophys. J. Int., 101, 425–478.

DeMets, C., R. G. Gordon, D. F. Argus and S. Stein, (1994). Effect of recent revisions to the geomagnetic reversal time scale on estimate of current plate motions, Geophys. Res. Lett., 21, 2191–2194.

Engdahl, E. R., R. D. Van der Hilst and R. P. Buland, (1998). Global teleseismic earthquake relocation with improved travel time and procedures for depth determination, Bull. Seis. Soc. Am., 88, 722-743.

Guzmn-Speziale, M. and J. F. Ni, (2000). Comment on "Subduction in the Indo-Burmese region: Is it still active?" by S. P. Satyabala. Geophys. Res. Lett. 27, 1065–1066.

Heck, N.H., (1947). List of seismic sea waves, Bull.Seism. Soc. Am., 37, 269-286.

Jaiswal R. K. and B. K. Rastogi, (2006). Tsumamigenic sources in the Indian Ocean, 6th Asian Seismological Commission (ASC) General Assembly – 2006, Symposium on Earthquake and Tsunami Disaster Preparedness and Mitigation, (Abstract Id O019, Session: Subduction Zone, Seismology and Tsunami), November 7-10, 2006 Bangkok, Thailand, pp 84-85.

Lay, T., H. Kanamori, C. J. Ammon, M. Nettles, S. N. Ward, R.C. Aster, S. L. Beck, S. L. Beck, M. R. Brudzinski, R. Butler, H. R. DeShon, G. Ekstrom, K. Satake and S. Sipkin, (2005). The Great Sumatran-Andaman earthquake of 26 December 2004, Science, 308, 1127–1133.

Lisitzin, E. (1974). Sea Level Changes, Elsevier Oceanographic Series, No.8, New York, 273pp.

Macmurdo, Captain, (1821). Account of the earthquake which occurred in India in June 1819, Edinburgh Phil. J., 4, 106-109.

Mathur, S. M., (1998). Physical Geology of India, National Book Trust of India, New Delhi.

McCloskey, J., Suleyman S. Nalbant and Sandy Steacy, (2005). Earthquake risk from coseismic stress, Nature, 434, 291.

Murty, T. S., A. Bapat and Vinayak Prasad, (1999). Tsunamis on the coastlines of India, Science of Tsunami Hazards, 17(3), 167-172.

Nalbant, Suleyman S., Sandy Steacy, Kerry Sieh, Danny, Natawidjaja and John McCloskey, (2005). Earthquake risk on the Sunda trench, Nature, 435, 756-757.

Natawidjaja, D. H., K. Sieh, S. N. Ward, H. Cheng, R. L. Edwards, J. Galetzka and B. W. Suwargadi, (2004). Paleogeodetic records of seismic and aseismic subduction from central Sumatran microatolls, Indonesia, J. Geophys. Res., 109, B04306, doi:10.1029/2003JB002398.

Natawidjaja, D. H., Kerry Sieh, Mohamed Chlieh, John Galetzka, Bambang W. Suwargadi, Hai Cheng, R. Lawrence Edwards, Jean-Philippe Avouac and Steven N. Ward, (2006). Source parameters of the great Sumatra megathrust earthquakes of 1797 and 1833 inferred from coral microatolls, J. Geophy. Res., 111, doi:10.1029/2005JB004025.

Nelson, Captain, (1846). Notice of an earthquake and a probable subsidence of the land in the district of Cutch, near the mouth of Koree, or the eastern branch of the Indus in June 1845, Geol. Soc. London, Quart. J., 2, 103.

Newcomb, K.R. and W.R. McCann, (1987). Seismic history and tectonics of the Sunda Arc, J. Geophys. Res., 92(B1), 421-439.

Oldham, T. A., (1833). Catalogue of Indian earthquakes, Mem. Geol. Surv. India, 19, 163 215.

Ortiz, M. and R. Bilham, (2003). Source area and rupture parameters of the 31 December 1881 Mw = 7.9 Car Nicobar earthquake estimated from tsunamis recorded in the Bay of Bengal, J. Geophys. Res., 108(B4), 2215, doi:10.1029/2002JB001941.

Pararas-Carayannis, G., (2003). Near and Far-Field Effects of Tsunamis Generated By the Paroxysmal Eruptions, Explosions, Caldera Collapses and Massive Slope Failures of The Krakatau Volcano in Indonesia on August 26-27, 1883, Science of Tsunami Hazards, 21(4), 191 222.

Pararas-Carayannis, G., (2007). The Earthquakes and Tsunami of September 12, 2007 in Indonesia Preliminary Report, http://www.drgeorgepc.com/Tsunami2007Indonesia.html

Pendse, C. G., (1948). The Makran earthquake of the 28th November 1945, India Met. Deptt. Scientific Notes, 10, 141-145.

Piatanesi A, S. Tinti and I. Gavagni, (1996). The slip distribution of the 1992 Nicaragua earthquake from tsunami run-up data, Geophys. Res. Lett., 23(1), 37-40.

Pollitz F. Fred, Paramesh, Banerjee, Roland Burgmann, Manabu Hashimoto and Nithiwatthn Choosakul, (2006). Stress changes along the Sunda trench following the 26 December 2004 Sumatra-Andamna and 28 March 2005 Nias earthquakes, Geophy. Res. Lett., 33, L06309, doi:10.1029/2005GL024558.

Rastogi, B. K., (2005a). Some facts about 26 Dec.2004 Sumatra earthquake & tsunami, http://www/bestindia.com/jgsi,17pp.

Rastogi, B. K., (2005b). Why did the 28 March 2005 Sumatra earthquake of Mw 8.7 generate only a minor tsunami, Curr. Sc. In., 89(5), 731-732.

Rastogi, B. K. and R. K. Jaiswal, (2005). Tsunamigenic sources in the Indian Ocean, Indian Geophysical Union (IGU), 42nd Annual Convention, 7-9 Dec. 2005, Barkatullah University, Bhopal, p 58-59.

Rastogi, B.K. and R.K. Jaiswal, (2006). A catalog of tsunamis in the Indian Ocean, Science of Tsunami Hazards, 25(3), 128-143.

Satyanarayana, H. V. S. and B. K. Rastogi, (2005). Assessment of possible tsunamigenic earthquakes in the Indian Ocean Region and earthquake hazard in the coastal region of India, Project proposal Proc. National Workshop on Formulation of Science Plan for "Coastal Hazard Preparedness", Group III: Seismicity, 18-19 February 2005, National Institute of Oceanography, Goa (www.nio.org/jsp/Science Plan/jsp).

Sieh, K., J. Rais and Y. Bock, (1991). Neotectonics and paleoseismic studies in west and north Sumatra (abstract), Eos Trans. AGU, 72(44), Fall Meet. Suppl., 460.

Stein, S. and E. A. Okal, (2005). Speed and size of the Sumatra earthquake, Nature, 434, 581–582.

Socquet, A., C. Vigny, W. Simons, N. Chamot-Rooke, C. Rangin and B. Ambrosius, (2006). India and Sunda plates motion and deformation along their boundary in Myanmar determined by GPS. J. Geophys. Res. 111 doi: doi: 10.1029/2005JB003877.

Subarya, C., M. Chlieh, L. Prawirodirdjo, J. P. Avouac, Y. Bock, K. Sieh, A. J. Meltzner, D. H. Natawidjaja and R. McCaffrey, (2006). Plate-boundary deformation associated with the great Sumatra-Andaman earthquake, Nature, 440, 46-51.

Tregoning, P., F. K. Brunner, Y. Bock, S. S. O. Puntodewo, R. McCaffrey, J. F. Genrich, E. Calais, J. Rais and C. Subarya, (1994). First geodetic measurement of convergence across the Java Trench, *Geophys. Res. Lett.*, *21*, 2135–2138.

Vigny, C., A. Socquet, C. Rangin, N. Chamot-Rooke, M. Pubellier, M.-N. Bouin, G. Bertrand and M. Becker, (2003). Present-day crustal deformation around Sagaing fault, Myanmar. J. Geophys. Res. 108(B11) doi: doi: 10.1029/2002JB001999.

Wang, K., R. D. Hyndman and M. Yamamoto, (1995). Thermal regime of the southwest Japan subduction zone: effects of age history of the subducting plate. Tectonophysics 248, 53–69.

Wiens, D.A., S. Stein, C. Demets, R.G. Gordon and C. Stein, (1986). Plate tectonic models for Indian Ocean "Intrplate" deformation, Tectonophy., 132, 37-48.

Zachariasen J., K. Sieh, F. W. Taylor, R. L. Edwards and W. S. Hantoro, (1999). Submergence and uplift associated with the giant 1833 Sumatran subduction earthquake: Evidence from coral microatolls, J. Geophys. Res., 104, 895-919.

Zachariasen J., K. Sieh, F. W. Taylor and W. S. Hantoro, (2000). Modern vertical deformation above the Sumatran subduction zone: Paleogeodetic insights from coral microatolls, *Bull. Seis. Soc. Am.*, *90*, 897-913.

Table 1. List of tsunamis generated due to earthquakes/volcanic eruptions that affected Indian region and vicinity in the Indian Ocean

S. N.	Date	Source/ Affected region	Long. °E	Lat. °N	Eq. Mag	Comment	Ref.
1	326 B.C.	Indus delta /Kutch region				Alexander's navy destroyed. Massive sea waves in the Arabian Sea due to large earthquake.	Lisitzin (1974)
2	416 AD	Java-Sumatra				Probably the 416 A.D. Krakatau eruption/explosion/collapse generated a series of catastrophic tsunamis affected Tamilnadu, which must have been much greater than those generated in 1883.	Rastogi & Jaiswal (2006)
3	500 AD	Poompuhar, Tamilnadu (probably due to Krakatau eruption)	79.52	11.12		Poompuhar town was a flourishing ancient town known as Kaveripattinam that was washed away due to tsunami generated probably due to Krakatau eruption	Rastogi & Jaiswal (2006)
4	900 AD	Nagapattinam Tamilnadu (may be from Sunda-Andaman arc)	79.53	10.46		Tsunami waves had washed away the Budhist monastery and several temples and killed hundreds of people. There is evidence of this in Kalaki Krishnamurty's book "Ponniyin Selvan- The Pinacle of Sacrifice".	Rastogi & Jaiswal (2006)
5	1008	Iranian Coast	60	25		Tsunami has been observed in the North Indian Ocean on the Iranian coast from a local earthquake.	Murty et al. (1999)
6	1524	Dabhol, Maharashtra	73.2	17		Tsunami due to a large earthquake caused considerable alarm to the Portugese fleet assembled in the area.	Bendick and Bilham, (1999)
7	May 1668	Samaji – Delta of Indus	68	24		The town of Samawani (or Samaji) sunk into the ground with 30,000 houses during an earthquake.	Oldham (1883)
8	1762.04.02	Bangladesh (Bay of Bengal)	92	22		The earthquake of Bangladesh also caused a tsunami in the Bay of Bengal. The water in the Hoogly River in Kolkata rose by two meters. The rise in the water level at Dhaka was so sudden that	Mathur (1988)

						hundreds of boats capsized and many people were drowned.	
9	1819.06.16	Kutch	71.9	26.6	Mw 7.8	The town of Sindri (26.6N 71.9E) and adjoining country were inundated by a tremendous rush from the ocean, and all submerged, the ground sinking apparently by about 5m	Macmurdo (1821)
10	1842.11.11	N. Bay of Bengal	90	21.5		Due to earthquake near the northern end of Bay of Bengal caused a tsunami by which waters of the distributaries of the Ganges Delta were agitated. Boats were tossed about as if by waves in a squall of wind.	Oldham (1883)
11	1845.06.19	Kutch	68.37	23.6	Mw 7.0	The sea rolled up the Koree mouth of the Indus overflowing the country as far westward as the Goongra river, northward to the vicinity of Veyre, and eastward to the Sindree Lake	Nelson (1846)
12	1847.10.31	Little Nicobar Island	93.667	7.333	Mw 7.5-7.9	Small island of Kondul (7¡13'N, 93¡42'E) near Little Nicobar was inundated by an earthquake whose Mw, magnitude could have been >7.5 (Bilham et al. 2005).	Berninghausen (1966), Heck, (1947)
13	1868.08.19	Andaman Islands	92.73	11.67			Rastogi & Jaiswal (2006)
14	May 1874	Sunderbans (Bangladesh)	89	22		Tsunami struck Sunderbans killing several hundred thousand people. It was result of an earthquake in Bhola district. Earthquake and tsunami both played havoc in vast areas of Sunderbans, 24-Prganas, Midnapore, Barishal, Khulna and Bhola. Even Kolkata felt its impact.	Rastogi & Jaiswal (2006)

15	1881.12.31	W. of Car Nicobar	92.43	8.52	Mw 7.9	Though tsunami run-ups and waves heights were not large; its effects were observed in the Andaman & Nicobar Islands (Port Blair, 1m) and were recorded on the east coast of India	Berningh ausen (1966), Ortiz and Bilham (2003)
						(Nagapatinam, 1.2m). Then tsunami struck Chennai, Vishakhapatnam, Mahanadi delta in Orissa and at Pamban in the Gulf of Mannar.	
16	Jan. 1882	Sri Lanka (may be from Indonesia)	81.14	8.34			Berningh ausen (1966)
17	1883.08.27	Krakatau (Volcanic Eruption)	105.25	-6.06		Due to Krakatau volcanic eruption of in Indonesia, 35m-high tsunami took a toll of 36,000 lives in western Java and southern Sumatra. Tsunami waves were observed throughout the Indian Ocean, the Pacific Ocean, the American West Coast, South America, and even as far away as the English Channel.	Berningh ausen (1966)
18.	1884	W. of Bay of Bengal				A tsunami was noticed at Dublet (mouth of Hoogly River) near Kolkata due to earthquake in the western part of the Bay of Bengal in 1884 that reached up to Port Blair.	Murty et al. (1999)
19.	1935.05.31	Andaman-Nicobar			Mw 7.5	Tsunami in SW Sumatra.	Rastogi & Jaiswal (2006)
20	1935.11.25	Andaman-Nicobar	94	5.5	Ms 6.5		Rastogi & Jaiswal (2006)
21	1941.06.26	Andaman Islands	92.5	12.1	Mw 7.7	Height of the tsunami was reported to be of the order of 0.75 to 1.25	Bilham et al.

						meters. This tsunami was witnessed along the eastern coast of India. It is believed that nearly 5,000 people were killed by the tsunami on the east coast of India.	(2005)
22	1945.11.27	Makran Coast	63.5	25.2	Mw 8.0	More than 4000 people were killed on the Makran Coast by both the earthquake and the tsunami. Max.run up 17m. The height of the tsunami in Mumbai was 2m. A total of 15 persons were washed away in Mumbai.	Murty et al. (1999)

23	1983.11.30	Chagos ridge	72.11	6.85	Mw 7.7	In the lagoon, on Diego Garcia, there was a 1.5-meter rise in tsunami wave height and there was some significant wave damage near the southeastern tip of the island. A 40 cm wave was also recorded at Victoria, Seychelles. There was a large zone of discolored seawater observed 60 - 70 km NNW of Diego Garcia.	Rastogi & Jaiswal (2006), NEIC
24	2004.12.26	Off west coast of N Sumatra and Andaman-Nicobar	95.947	3.307	Mw 9.3	The 2004 Sumatra-Andaman earthquake of magnitude 9.3 generated 30m-high tsunami near the Andaman-Nicobar region. It was the deadliest tsunami killing about 300.000 people in 13 countries situated all around the Indian Ocean. The earthquake produced large landslides that were also cause of generating destructive tsunami.	http://www/bestindia.com/jgsi,17pp. & Rastogi (2005b)
25	2005.03.28	Off west coast of N Sumatra	97.013	2.074	Mw 8.7	2005 tsunami was only locally damaging. A 3-meter tsunami damaged the port and airport on Simeulue. Tsunami runup heights as high as 2 meters were observed on the west coast of Nias and 1 meter at Singkil and Meulaboh, Sumatra.	Rastogi (2005) & NEIC
26	2007.09.12	Off west coast of S Sumatra	101.374	-4.52	Mw 8.4	Killing 9 people and injured few tens, generated relatively small tsunami near epicentral zone.	George, P.-C. (2007),

Abbreviation: MAK - Makran Accretion Zone, MUR – Murray Ridge, OWE – Owen Fracture Zone, CAR – Carlsberg Ridge, CHA – Chagos Archipelago, A & N – Andaman & Nicobar Islands, SUM – Sumatra, NIN – Ninety East Ridge, SUN – Sunda Subduction Zone and JAVA-Java.

GEOLOGICAL EVIDENCE FOR PALEO-TSUNAMIS IN SRI LANKA

Kapila Dahanayake and Nayomi Kulasena

Department of Geology, University of Peradeniya,
Peradeniya 20400, Sri Lanka.
(e-mail: kapidaha@hotmail.com)

ABSTRACT

After the 2004 Indian Ocean tsunami inundation event, thin sediment films of fining up sequences were located in several topographic depressions of the southern coastal belt of Sri Lanka. The films consisting of silty fine sand with particular microfossil assemblages were located also in closed containers, bottles and kitchen tables. Well preserved microfossils such as foraminifera, radiolarians as well as spicules of sponges were noted in these recent tsunami sediments.

Random augur holes were drilled into some selected depressions in the southern coastal villages of Peraliya and Denuwala situated at locations separated by about 50km. In several such holes, at least two fining up sequences were located below the surface in soil horizons separated from each other by 35cm to 1m. These soil profiles were overlying older coral reefs developed on lateritic formations. The microscopic observations on particular size fractions of the soil horizons showed microfossil assemblages with textures, color and organic C contents strikingly comparable to those observed in the recent tsunami sediments of Sri Lanka. Our findings imply the occurrence of at least two paleo-tsunami events of different ages in Sri Lanka originating apparently from a common source.

Science of Tsunami Hazards, Vol. 27, No. 2, page 54 (2008)

1. INTRODUCTION

The undersea tsunamigenic Sumatra-Andaman Indian Ocean earthquake occurred in the morning of 26 December 2004 off the west coast of northern Sumatra registering a magnitude of 9.3 on the Richter Scale (Kruger and Ohrnberger 2005). The tsunami caused enormous destruction to life and property in many countries of the Indian Ocean with over 35,000 deaths recorded in southern, eastern and northern Sri Lanka. Massive tsunami waves with a wave height varying from 3 to 11m moved inland with speeds of about 30 to 40 km per hour through the southern, eastern and northern beaches (Liu et al. 2005; Tanioka et al. 2004 and Wijetunge 2006). These waves brought with them long trains of water carrying dark colored suspensions of fine grained materials from ocean environments. The villagers of Peraliya and Denuwala from the southern coastal belt reported at least three episodes of waves. A few hours later, tsunami waters had receded or were absorbed by the underlying soils leaving behind at least three types of sediments in the highly populated southern coastal zone as follows: (i) A typical sequence of such sediments would show a basal layer of scoured coastal sediments of varying size with debris and artifacts as big as vehicles. (ii) In the middle part of such a sequence, visible mostly in uninhabited beaches, can be observed sandy sediments with signatures of oscillating bidirectional currents developed during final stages of the event due to deposition through gradients in transport (iii) The upper part of a tsunami sedimentary sequence can be interpreted as a calm condition after a tsunamigenic earthquake and it shows fine grained clayey sediments. This unit shows upward fining due to sediment falling out of suspension (Bondevik et al.). These sediments suggest waning flow or pre-backwash deposition.

Preliminary microscopic studies of the sediments showed prolific occurrence of microfossils- that was considered an important signature of tsunami sediments- supported by characteristic cumulative curves. Microfossil assemblages (ostracods, diatoms, foraminiferans and pollen) provide evidence of sediments transported and deposited by tsunamis (Hickman et al., 2001; Prendergast, 2006). Analysis of Dec. 26/04 tsunami sediments collected along Karaikal to Nagapattinam beaches in Tamilnadu, India had revealed a thin cover of silty clay lithology consisting of foraminiferal assemblages. (Satyanarayana et al., 2007). Foraminiferan assemblages reflect the characters of tsunamis such as their direction and coastal topography. The well-preserved benthic assemblages in India are believed to have come from an inner shelf habitat with bathymetry less than 30m (Nagendra et al. 2006). Deep-sea foraminiferal facies indicate the source of particles transported by the tsunami (Uchida et al. 2005). Foraminiferal assemblages can differentiate pre-tsunami sediments from tsunami lain sediments (Hawkes et al. 2006). Historical texts of Sri Lanka refer to at least two past tsunami events that had occurred between 2000 to 3000 B.C (Geiger 1934; Suraweera 2000; Stoddart 2005; Dahanayake 2006). The purpose of the present study is to investigate potential paleo-tsunami horizons located in some soil profiles of the southern coastal region of Sri Lanka.

2. METHODS OF STUDY

Samples of both recent and paleo-tsunami sediments were collected from the Southern coastal belt of Sri Lanka. Recent samples were collected from selected locations such as closed offices, containers

where the recent tsunami waters had found their way via openings. Samples were also collected from kitchen tables and open bottles located/stacked at heights of about 50cm above the ground surface which were preferred sites for deposition of tsunami sediments (Dahanayake 2006). Random drilling of selected depressions was done in the coastal villages of Peraliya and Denuwala (Fig.1) where recent tsunami sediments had preferentially accumulated. This led to the discovery of soil profiles with at least two stratigraphic horizons containing possible paleo-tsunami sediments. These were so identified due to the comparable grain size distribution, microfossil content, Organic C and Calcium Carbonate contents, color and texture as in known recent tsunami sediments. In these older sedimentary deposits the fining upward character was also observed.

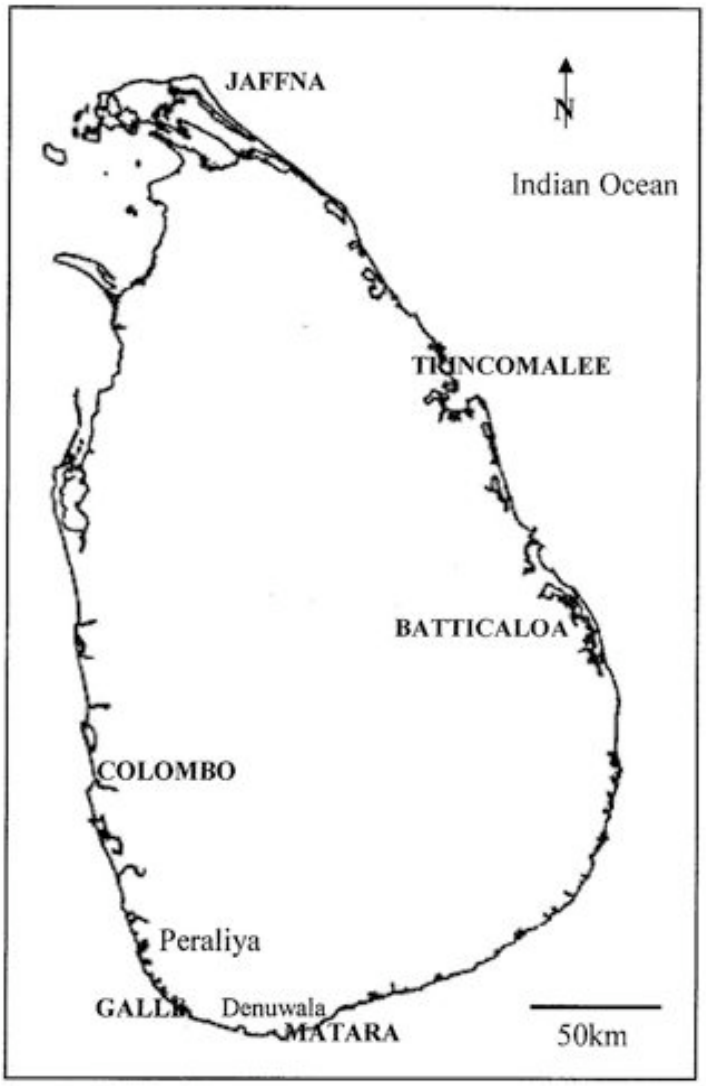

Fig. 1- Map of Sri Lanka showing the locations of the coastal villages of Peraliya and Denuwala

Sediment samples collected from sites described above as well those from storm surge and near shore deposits were air dried and grain size analysis was done using 1mm, 0.5mm, 0.25mm, 0.212mm, 0.125mm, 0.063mm sieves. Cumulative curves (as in Tickell, 1965) were constructed for typical samples from each sampling site from the 2004 tsunami (Fig.2, Fig. 3A) and for the upper and lower brownish layer from each augur hole sample site (Fig.2, Fig. 3B, C). All of the 2004-tsunami samples were scanned for microfossils in each size fraction using a reflected-light microscope. At every site, the 0.125 fraction contained the highest concentration of microfossils. Therefore only that size fraction was used for more detailed identification of microfossils using LEO 1420 VP Scanning Electron Microscope (SEM) on gold-sputtered mounts. This was done with typical selected samples from each 2004 tsunami site and both layers of each augur hole site.

Fig. 2- Dug pit profile at Peraliya showing the Recent (TS3) and Paleo-tsunami (PTS 1, 2) horizons. Note the characteristic yellowish brown coloration of tsunami sediments

3. RESULTS

Several randomly selected soil profiles located at about 100m inland from the southern coast were studied. The locations of the profiles were at the coastal villages of Peraliya and Denuwala situated 50 km apart (Figs. 1 & 2). The profiles show comparable horizons as follows: (Top to Bottom) A-

Relatively thin yellowish brown horizon of Recent tsunami sediments; B- Black clayey calcareous humic soil; C-thin yellowish brown Paleo-tsunami (?) horizon; D- Black clayey calcareous humic soil; E- Yellowish brown clayey fine sand paleo-tsunami (?) horizon; F- Mollusc-rich Coral Reef; G-Lateritic bedrock.

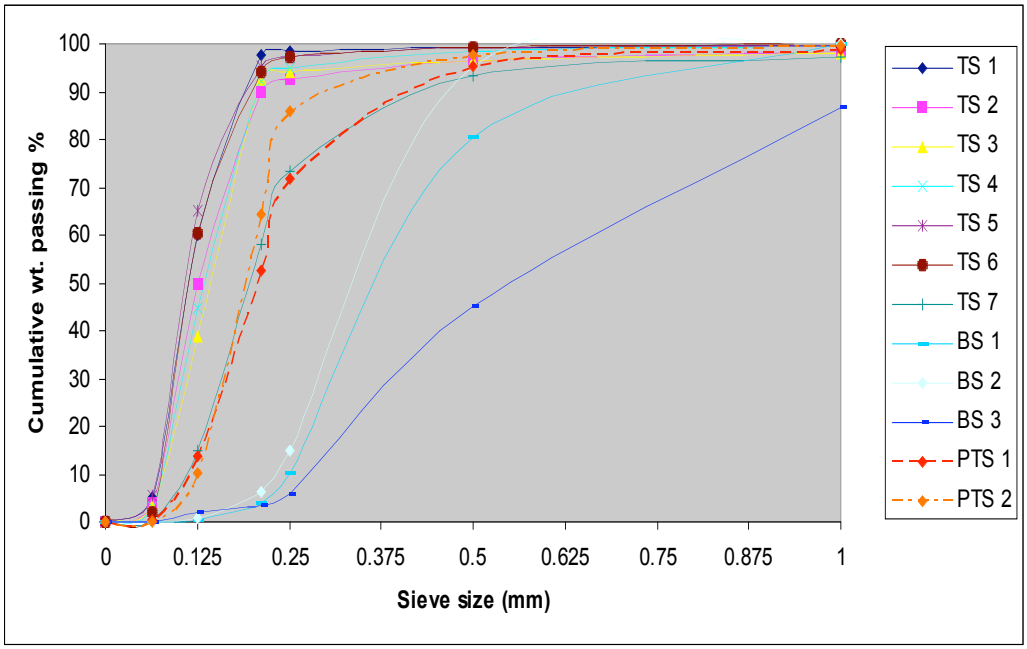

Fig. 3- The diagram showing the grain size distribution curves of Recent Tsunami sediments (TS 1-7), Paleo-tsunami sediments (PTS 1-2) and Beach sand (BS 1-3). Note the comparable grain size distributions of Recent and Paleo-tsunami sediments.

Detailed observations on horizons given in Figures 2 and 4 reveal there is a high concentration of well-preserved microfossils in the thin yellowish brown horizons. The microfossils found in the recent known tsunami sediments show striking similarities to those of the Paleo-tsunami sediments reported here. The types of microfossils are comparable and organic C of all the thin horizons lies between 1.9 to 2.7 %. Their texture and color are comparable to those deposited during Dec 26/04 tsunami inundation event. Microfossils are rarely observed in the humic horizons which have relatively high organic C contents (6 to 8 %). The soil profiles in the study areas overlie coral limestone formations.

a) Both sediment types studied were brownish yellow in color and of fine sand size generally showing a fining upward trend in the field. Cumulative curves of both types of sediments showed comparable grain size distributions. Similar trends were noted for all the paleo-sediment samples studied. It is interesting to note that the cumulative curve for the 2004 tsunami sediment (TS 7 in Fig. 3) from the **arrack** bottle (Dahanayake, 2006) and those for the paleo-tsunami sediments studied (PTS 1 to PTS 2 in Fig. 3 showed strikingly similar trends.

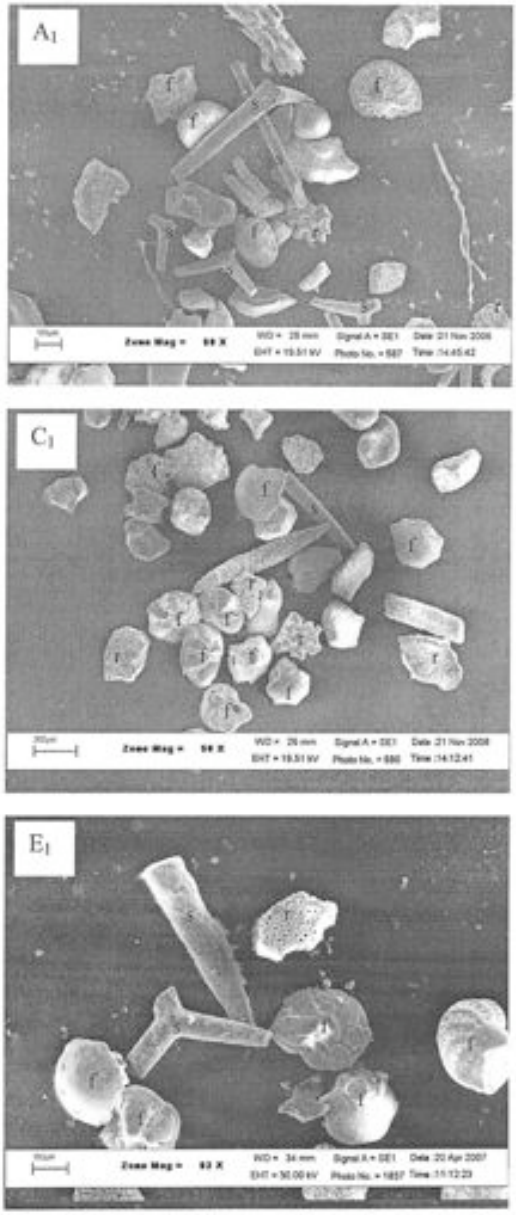

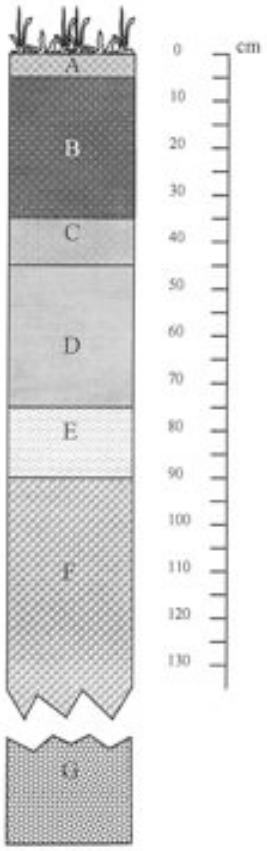

Fig. 4- Soil Profile at Peraliya

Description of Horizons in the Soil Profile

A- Yellowish brown Recent tsunami sediment with clayey fine sand with small mollusk tests –fining upward character observed

B- Black clayey calcareous humic soil with coarse weathered rock fragments

C- Paleo-tsunami horizon with clayey fine sand underlain by coarser layer rich in small mollusk tests- fining upward character observed

D- Black clayey calcareous soil with soil coated small mollusks.

E- Paleo-tsunami horizon with yellowish brown clayey fine sand underlain by coarser layer rich in mollusk tests

F- Mollusk rich reef G- Lateritic Bedrock

A_1, C_1 & E_1 are photomicrographs showing microfossil assemblages found in soil horizons A, C & E respectively ***- s- spicules of sponges; f-foraminifera and r-radiolaria***.

b) In both types of sediments, assemblages of microfossils as well as sub rounded quartz grains were found more or less exclusively on the fraction retained on the 0.125 mm sieve (Fig. 3).

c) The above observations highlight the similarities of both 2004 tsunami and paleo-tsunami sediments collected from the Southern coastal region of Sri Lanka in grain size distribution as well as microfossil contents.

4. DISCUSSION AND CONCLUSIONS

The microfossil content, textural and compositional attributes of Recent tsunami sediment samples collected from various locations were strikingly similar to those sediment horizons lying at depths ranging from 35cm to 1m in the soil profiles studied. These observations suggest (a) at least two past tsunami events and (b) the arrival of tsunami waters across a common source area which had been agitated due to breaking of tsunami waves in a relatively shallow ocean environment. The similarity of texture, color and composition with comparable microfossil assemblages of radiolarians, foraminiferans, and diatoms in both recent and older sediment layers suggest a paleo -tsunami origin for the older stratigraphic horizons. At least two such events are represented in the soil profiles studied. There are references in ancient texts such as Jataka Stories and others to paleo-tsunamis in the Indian Ocean and the present observations confirm such historical observations. Currently efforts are under way to determine radiocarbon dates for stratigraphically older horizons represented in the soil profiles studied.

Acknowledgements

The authors wish to thank Prof. Atula Senaratne, Dr H.M.T.G.A.Pitawala, Dr Ms. Sudharma Yatigammana - colleagues of one of us (K.D) at the Departments of Geology and Zoology of the Faculty of Science, University of Peradeniya for their assistance in analyzing the samples and identification of microfossils. Ms Sepa Nanayakkara, Research Officer at the Industrial Training Institute (ITI), Colombo kindly assisted with SEM studies. Ms Menaka Hindagolla, Senior Assistant Librarian at the University Library of Peradeniya helped in bibliographic searches. Finally the kindness of the villagers of tsunami-stricken southern coastal region of Sri Lanka is remembered with gratitude. A generous research grant (RG/2005/DMM/05) for one of us (K.D) from National Science Foundation (NSF) of Sri Lanka is gratefully acknowledged.

5. REFERENCES

Dahanayake, K. (2006) Science at the Solstice: A day in the life of a scientific planet, Abstract on Tsunami sediments. Nature, v.441, pp.1040-1045.

Geiger, W. (Translator), (1934) *The Mahawamsa* (The Great Chronicle of Ceylon-Sri Lanka) Oxford University Press London, (in Sinhala).

Hickman, C. P., Roberts, L. S., Larson, A. (*2001*) Integrated Principles of Zoology. McGraw-Hill New York

Kruger, F., Ohrnberger, M. (2005) Tracking the rupture of the M_w = 9.3 Sumatra earthquake over 1150km at teleseismic distance, Nature, v.435, pp.937-939.

Liu, P.L.F., Lynett, P., Fernando, H., Jaffe, B.E., Fritz, H., Higman, B., Morton, R., Goff, J., Synolakis, C. (2005) Observations by the International Tsunami survey Team in Sri Lanka. Science, v.308, p.1595.

Nagendra, R., Kamalak Kannan, B.V., Sajith, C., Sen, G., Reddy, A.N., Srinivasalu, S. (2005) A record of foraminiferal assemblage in tsunami sediments along Nagappattinam coast, Tamil Nadu. Curr. Sci., v.89, pp.1947-1952.

Prendergast, A. (2006) Echoes of ancient tsunamis. AusGeo News #83.

Satyanarayana, K., Nallapa Reddy, A., Jaiprakash, B.C., Chidambaram, L., 2007. A note on foraminifera, grain size and clay mineralogy of tsunami sediments from Karaikal-Nagore-Nagapattinam beaches, Southeast Coast of India. Journal Geological Society of India, v.69, pp.70-74

Stoddart, J. (2005) Tidal waves in Ceylon resulting from the Eruptions in the Straits of Sunda, August 1883. Surveyor General's Report, Ceylon (Sri Lanka). Island Newspaper, Sri Lanka Feb. 15.

Suraweera, A. V. (2000) Rajavaliya- A Comprehensive account of the kings of Sri Lanka. Vishvalekha Publication, Sri Lanka.

Tanioka, Y., Nishimura, Y., Hirakawa, K., Imamura, F., Abe, I., Abe, Y., Shindou, K., Matsutomi, H., Takahashi, T., Imai, K., Harada, K., Namegawa, Y., Hasegawa, Y., Hayashi, Y., Nanayama, F., Kamataki, T., Kawata, Y., Fukasawa, Y., Koshimura, S., hada, Y., Azumai, Y., Hirata, K., Kamikawa, A., Yoshikawa, A., Shiga, T., Kobayashi, M., Masaka, S. (2004) Tsunami run-up heights of the 2003 Tokachi-oki earthquake. Earth Planet Space, v.56, pp.359-365.

Uchida, J., Abe, K., Hasegawa, S., Fujiwara, O., Kamataki, T., Irizuki, T., Hirakawa, K. (2005) Characteristics of Faunal Succession of Foraminifera in Tsunami-deposits and Recognition of Sauce Area of Particles- A Case Study of the Holocene Tsunami Deposits at Tateyama, Southern Part of the Boso Peninsula, Central Japan. Abstract American Geophysical union-#T11A-0361.

Wijetunge, J.J. (2006) Tsunami on 26 December 2004: Spatial distribution of tsunami height and the extent o inundation in Sri Lanka. Science of tsunami hazards, v.24, pp.225-239.